

Paleogeographic numerical modelling of marginal seas for the Holocene – an exemplary study of the Baltic Sea

Jakub Miluch^{1,2}, Wenyan Zhang¹, Jan Harff³, Andreas Groh⁴, Peter Arlinghaus¹, Celine Denker¹

¹Institute of Coastal Systems – Analysis and Modeling, Helmholtz-Zentrum Hereon, Geesthacht, 21502, Germany

⁵5 Polish Geological Institute – National Research Institute, Marine Geology Branch, Gdańsk, 80328, Poland

³Institute of Marine and Environmental Sciences, University of Szczecin, Szczecin, 70-453, Poland

⁴Institute of Planetary Geodesy, Technical University Dresden, 01062, Germany

10 *Correspondence to:* Wenyan Zhang (wenyan.zhang@hereon.de); Jakub Miluch (jmilu@pgi.gov.pl)

Abstract. Sustainable management of marginal seas is based on a thorough understanding of their evolutionary trends in the past. Paleogeographic evolution of marginal seas is controlled by not only global and regional driving forces (eustatic sea level change and isostatic/tectonic movements) but also sediment erosion, transport, and deposition at smaller scales.

Consistent paleogeographic reconstructions at a marginal sea scale considering the global, regional and local processes is yet

15 to be derived, and this study presents an effort towards this goal. We present a high-resolution ($0.01^\circ \times 0.01^\circ$) paleogeographic reconstruction of the entire Baltic Sea and its coast for the Holocene period by combining eustatic sea-level change, glacio-isostatic movement, and sediment deposition. Our results are validated by comparison with field-based reconstructions of RSL and successfully reproduce the connection/disconnection between the Baltic Sea and the North Sea during the transitions between lake and sea phases. A consistent map of Holocene sediment thickness in the Baltic Sea has
20 been generated, which shows that relatively thick Holocene sediment deposits (up to 36 m) are located in the southern and central parts of the Baltic Sea, corresponding to depressions of sub-basins including the Arkona Basin, the Bornholm Basin as well as the Eastern and Western Gotland Basins. In addition, some shallower coastal areas in the southern Baltic Sea also host locally confined deposits with thickness larger than 20 m and are mostly associated with alongshore sediment transport and formation of barrier islands and spits. In contrast to the southern Baltic Sea, the Holocene sediment thickness in the
25 northern Baltic Sea is relatively thin and mostly less than 6 m. Morphological evolution of the Baltic Sea and its coastline is featured by two distinct patterns. In the north-eastern part, change of the coastline and offshore morphology is dominated by regression caused by post-glacial rebound that outpaces the eustatic sea level rise, and the influence of sediment transport is very minor, whereas a transgression together with active sediment erosion, transport and deposition have constantly shaped the coastline and the offshore morphology in the south-eastern part, leading to formation of a wide variety of coastal
30 landscapes such as barrier islands, spits and lagoons.

1. Introduction

The majority of the Earth's coasts and shelf seas are experiencing dramatic morphological changes as a result of joint effects of natural processes and anthropogenic activities (Mentaschi et al., 2018). Coasts of marginal seas composed of erodible soft material (sands, mud and moraine) are most variable in this context (Harff et al. 2017; Luijendijk et al., 2018; 35 Hulskamp et al., 2023). At short time scales, their morphology is constantly reshaped by atmospheric and oceanic forcing such as winds, tides and waves, and human interventions (Zhang et al., 2011a; Mentaschi et al., 2018; Weisse et al., 2021). At longer time scales, climate change-induced oscillations of sea level, ice-cover/retreat, isostatic/ tectonic movements and 40 variations in sediment supply from coastal erosion as well as riverine transport, exert a major control on morphological development of marginal seas (Zhang and Arlinghaus, 2022). In the forthcoming centuries, relative sea-level rise will 45 increasingly influence coastal morphological change and challenge the defense of coastlines. Sustainable management of marginal seas therefore requires a thorough understanding of the past and future morphological trends of evolution (Hulskamp et al., 2023). Management strategies need to consider the “geo-environmental” change in the past and future to separate natural and anthropogenic driving forces (Neumann et al., 2015) and understand their interplay. Learning from paleo-geomorphological history, particularly the post glacial period, will help to understand the coastal change in future (Harff et al., 2017).

Paleogeographic evolution of marginal seas is strongly associated with global and regional driving forces. Climatically controlled eustatic changes (Gale et al., 2002; Berra et al., 2010) interplay with regional settings such as 50 tectonics (Watts 1982; Vött 2007), isostasy (Peltier 1999, 2007; Lambeck et al., 2010, Spada et al., 2012) or even local factors like sediment availability and dynamics (Einsele 1996). Combination of these overlapping forces influences the relative sea level and may lead to significantly different coastal behaviours in various sections of marginal seas due to spatial 55 heterogeneity of described forces intensity (Rosentau et al., 2021).

Most paleogeographic reconstructions of marginal seas are based on a reversal of relative sea level composed of eustatic sea level change plus tectonic and glacio-isostatic crustal effects (Uehara et al., 2006; Harff et al., 2007; Yao et al., 2009; Sturt et al., 2013). A few studies have additionally incorporated sediment relocations based on interpolation techniques 55 and information from dated sediment cores, but are limited to local areas (Zhang et al., 2014; Xiong et al., 2020; Karle et al., 2021). This study presents a high-resolution numerical paleogeographic reconstruction of the entire Baltic Sea and its coasts for the Holocene period as a set of paleo-Digital Elevation Models, by taking into account not only eustatic sea-level change and glacio-isostatic movement but also sediment deposition. As such, this work represents a further step for comprehensive 60 paleogeographic reconstruction of marginal seas resolving spatial heterogeneity of driving forces across multi-scales. Our motivation is twofold: first to depict the morphological evolution of a complex marginal sea system in response to the impact of climate change and oceanic sedimentation; second, to provide a sediment budget analysis of the marginal sea for the Holocene period and compare with present-day sediment fluxes from land to the sea to disentangle natural and anthropogenic impacts.

2. Geological setting

65 The Baltic Sea is a semi-enclosed intra-continental marginal sea, connected with the North Sea through the Danish Straits (Rosentau et al., 2017). In terms of regional tectonics, the Baltic Sea Basin bridges between the Eastern European Platform Craton (EEC) consisting of the Fennoscandian (Baltic) Shield (BS) in the northeast and the Russian East European Platform (EEP) in the southeast and the Central Western European Platform Basin System in the southwest (Maystrenko et al., 2008). The Eastern and Western European Platform are separated by the deep NW-SE striking tectonic fault system of
70 the Tornquist-Teisseyre Zone (TTZ) and its northwestern prolongation, the Sorgenfrei-Tornquist Zone (STZ) (Uścinowicz 2014). Northeast of this zone, Precambrian crystalline rocks of the Baltic Shield and undeformed Phanerozoic sediments of the Russian Plate EEP on Precambrian basement form the coastal frame of the Baltic Sea. West of the TTZ, the Central Caledonides and Variscides together form the deep sedimentary basin of the Central European Depression filled mainly with
75 Paleozoic and Mesozoic deposits on a basement at depth of up to depth of 10-15 km (Uścinowicz 2014). The lowlands are mainly covered by Pleistocene sediments consisting of glacial, glacio-fluviatile and lacustrine deposits. The Holocene sediment is represented by coastal, lacustrine and brackish marine deposits (Rosentau et al., 2017). Glaciers have shaped the surface of the mainland surrounding the Baltic Sea, as well as the Baltic Sea Basin itself (with an average water depth of 55 m) where they formed a series of sub-basins separated by shallower sills (Hall and van Böckel 2020). The Danish Straits connect the Baltic Sea with the North Sea through the Kattegat. Humid climate and a positive water balance promote an
80 estuarine circulation and a stratified water body with remarkable vertical and horizontal differences in salinity, density, and temperature in the present-day Baltic Sea (Matthäus and Franck, 1992; Wulff et al., 1990).

85 Advance and retreat of glacier during the Quaternary glacial cycles have caused a change of isostatic loading and unloading of the Baltic Basin's crust leading to a cyclicity in vertical crustal movement correlated to the climate cycles. The relationship between the vertical crustal movement and the sea-level change determines the hydrographic communication between the open North Sea and the Baltic Basin. The parts connecting the Baltic Basin and the North Sea thus serve a function of "gate" that is opened or closed by eustacy-isostacy-ice interaction. Correspondingly, the paleogeographic history of the Baltic Basin during the Quaternary was ruled mainly by the glacial cycles following the Milankovitch cyclicity. However, because of the erosional effects of the advancing ice sheet, sediments reflecting the geological history by proxy-data remained scarcely from the pre-glacial period. Andrén et al. (2011) have depicted this postglacial history based on
90 interpretation of proxy data including basin sediments and markers of paleo-coastlines by a set of paleogeographic maps (Fig. 1) which are used in our study for qualitative assessment of the results achieved by numerical modeling.

95 The evolution of the Baltic Sea since the Last Glacial Maximum is characterized by shifts between fresh water and marine sedimentary environments (Andrén et al., 2011). Starting from 16 kyr BP the Baltic Ice Lake (BIL) was formed in front of the retreating ice sheet filled with glacial melt water. Initially the water level in the lake was similar to global sea level and the melt water discharged to the Baltic Basin was flowing through the straits into the North Sea. The connection was however ceased due to glacio-isostatic uplift of the straits area at around 14 kyr BP (Björck, 2008). Another re-

connection occurred at ~13 kyr BP via the Central Swedish Lowlands as a result of rising water level caused by meltwater discharge to the BIL, but was interrupted by a short cooling phase of the Younger Dryas at ca. 12.8 kyr BP that caused glacial re-advance (Björck, 1995). As the influence of the isostatic uplift of the Baltic Shield prevails, the Baltic Basin remained disconnected from the North Sea (Fig. 1) until the late stage of the BIL. Glacier retreat and global sea-level rise reopened the gate connecting the Baltic Basin and the North Sea via the Central Swedish Lowlands (Fig. 1), initiating the brackish Yoldia Sea stage at ~11.7 kyr BP (Heinsalu and Veski, 2007). At ~10.7 kyr BP, isostatic uplift again re-closed the gate of the Swedish Depression (Fig. 1) and the Baltic Basin turned to a freshwater (lake) environment again (Sohlenius et al., 2001). The initial Ancylus Lake stage was characterized by a rising water level because of meltwater discharge from ice sheet until reaching a peak at ~10.5 kyr BP. Afterward a decrease of the water level occurred because of a drainage to the North Sea (Lemke et al., 2001; Rosentau et al., 2013). The climate-controlled Holocene sea-level rise in connection with the deforming lithospheric bulge surrounding the Baltic Shield re-opened the gate at the straits leading to the Littorina Transgression starting at ~8.0 kyr BP (Fig. 1). Since then, the water level in the Baltic Sea has been aligned with the sea level in the open North Sea until present day.

110

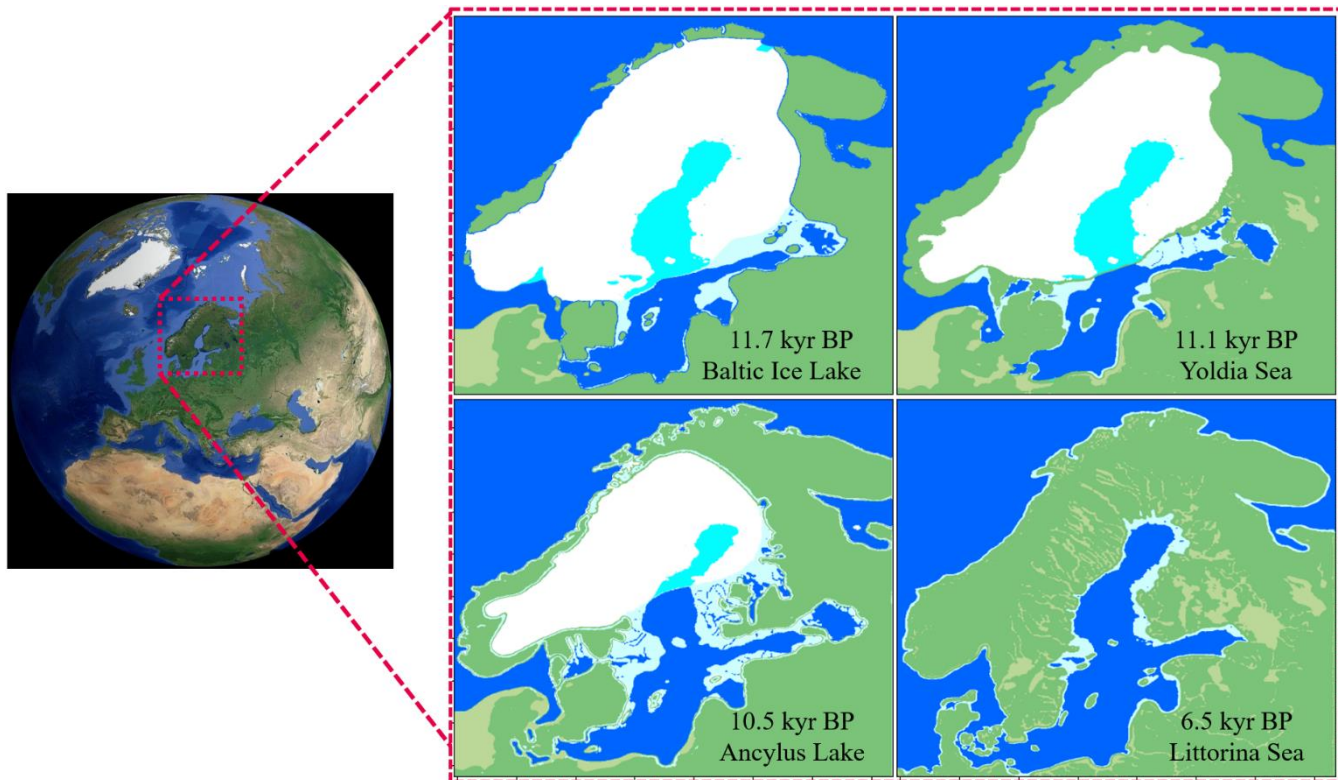


Figure 1: Location of the Baltic Sea (© Google Earth Pro) and paleogeographic maps (modified after Andrén et al., 2011) representing different Holocene stages of the Baltic Sea, including the Baltic Ice Lake/Yoldia Sea transition at 11.7 kyr BP, 115 the Yoldia Sea (end of the brackish phase) at 11.1 kyr BP, the Ancylus Lake (maximum transgression) at 10.5 kyr BP, and the Littorina Sea (most saline phase) at 6.5 kyr BP. Ice cover is shown by the mask in white, blue color stands for water, cyan corresponds to present-day water, green marks the land, whereas olive marks land in the past.

3. Data and methods

The main target of this study is the generation of a set of paleo-digital elevation models (paleo-DEMs)

120 corresponding to a high spatio-temporal resolution (0.01×0.01 degree and 500-years interval) reconstruction of the Baltic Sea evolution during the Holocene. Such reconstruction plays a critical role for the purpose of basin analysis (Allen and Allen, 2008), visualization of the past states of marginal seas (Xiong et al., 2020), morphogenetic interpretation (Miluch et al., 2021, Miluch et al., 2022) as well as hydro-morphodynamic modeling of circulation and sediment transport systems (Zhang et al., 2020). Since our reconstruction covers only a relatively short geological time span, i.e. from the initial stage of 125 the Holocene (11.7 kyr BP) till present day, the key influencing factors considered include eustatic sea level change, isostatic vertical crust movements and sediment deposition. Other factors such as sediment compaction play a secondary role at such time scale (Schmedemann et al., 2008) and therefore are neglected here. The equation following Harff et al. (2017) was applied to generate the paleo-DEMs for any specific time t during the Holocene with reference to present day ($t = 0$):

$$DEM_t = DEM_0 - \Delta RSL + \Delta SED, \quad (1)$$

130 where DEM_t is the paleo-digital elevation model at time t , DEM_0 is the present-day DEM, ΔRSL is the relative sea-level change and ΔSED is the change of sediment thickness by deposition. Integration of sediment thickness marks the major difference between our reconstruction and existing reconstructions.

The relative sea-level change ΔRSL is calculated by:

$$\Delta RSL = \Delta EC + \Delta GIA, \quad (2)$$

135 where ΔEC is the eustatic sea-level change and ΔGIA refers to the Glacial Isostatic Adjustment at time t with reference to present-day conditions.

After successful application of the equations in the South China Sea by Yao et al. (2009) and Xiong et al. (2020), we apply them for the first time to the Baltic Basin considering not only GIA and sediment accumulation but also differences in eustatic sea level and the water level in a regional basin following temporarily a separate regional hydrographic regime 140 when it is disconnected from the open sea.

During brackish-marine stages, the sea level of the Baltic basin follows that of the North Atlantic. EC in these stages thus reflects the global (eustatic) sea level. During lake stages, EC reflects the level of the freshwater lake that is fed by precipitation, ice's meltwater and rivers. In this case, EC in the coast of Fennoscandia influenced by the open ocean is modeled separately from that in the Baltic Basin.

The reconstructed DEMs were plotted using Golden Software Surfer 18 program. The software allows to visualize surface relief with pre-defined spatial resolution (Bola and Kayode, 2014; Libina and Nikiforov, 2020), perform grid-on-grid mathematical operations (Liu et al., 2020) as well as interpolate the data (Gonet and Gonet, 2017; Razas et al., 2023; Yilmaz 2007), and therefore acts as a convenient, widely-used tool in basin analysis (Covington and Kenelly, 2018; Grund and Geiger, 2011). The general workflow for data collection, synthesis and interpretation is depicted in Fig. 2.

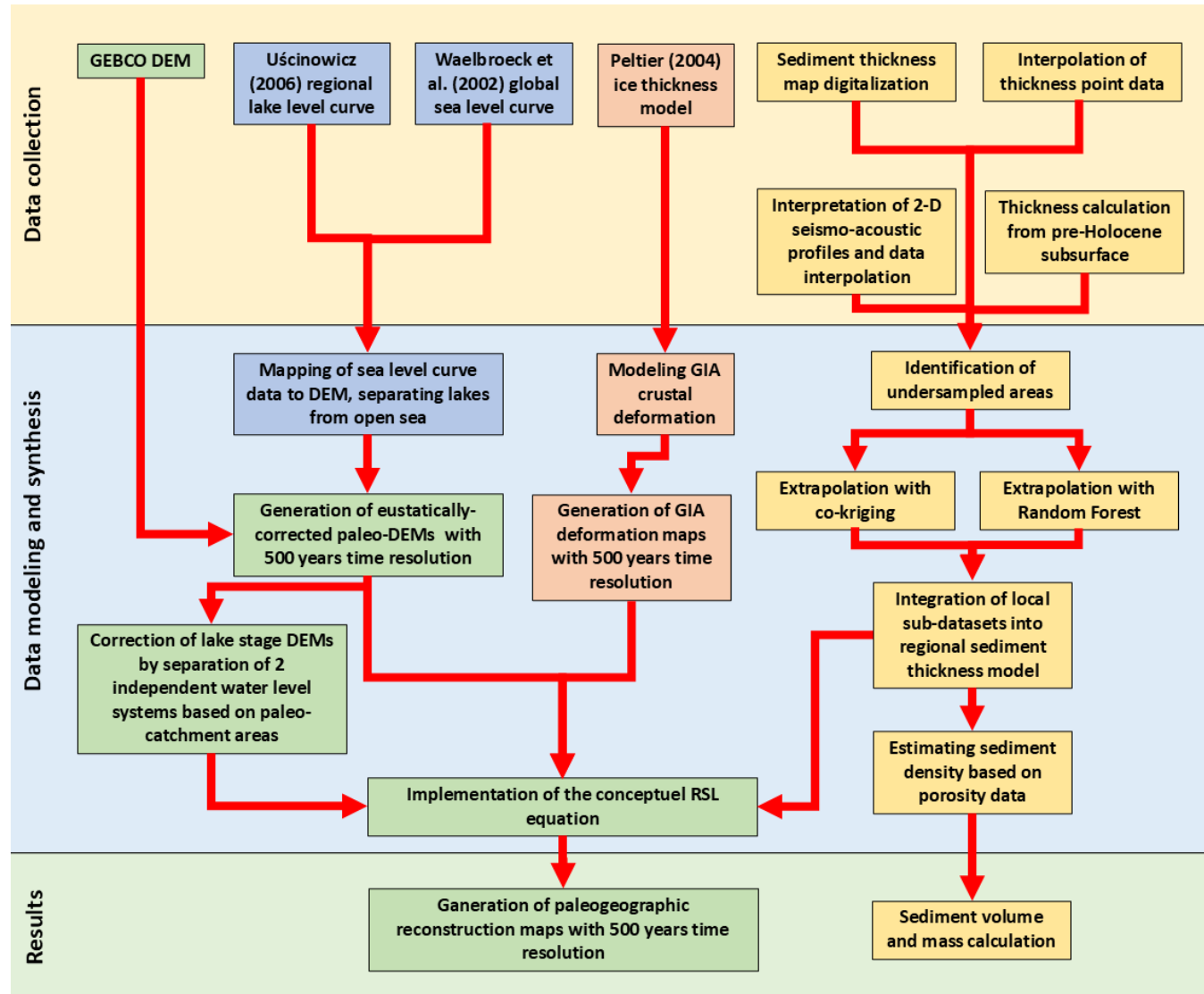


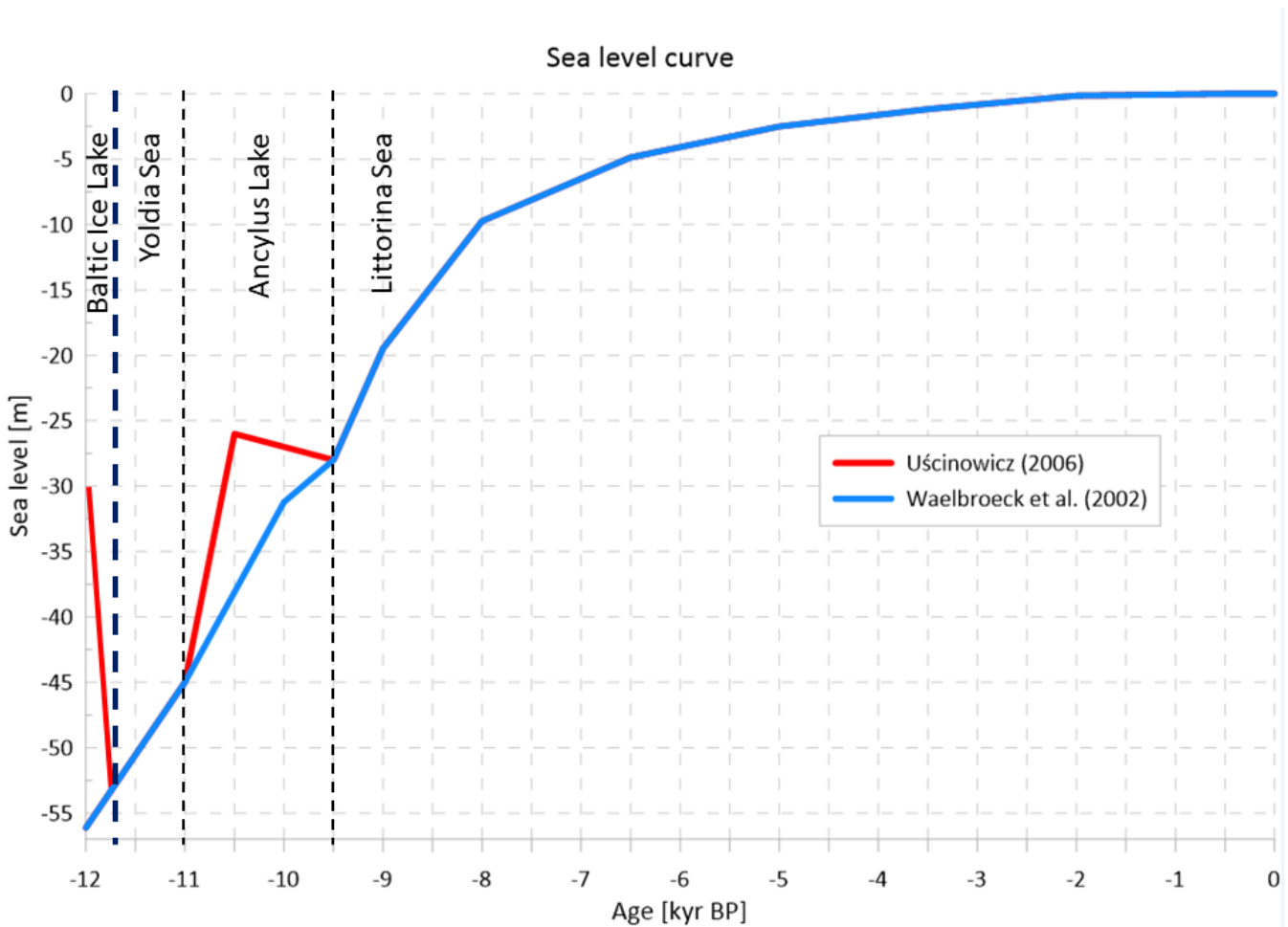
Figure 2: General workflow chart for data collection, synthesis and interpretation.

3.1. Digital Elevation Model (DEM₀)

The present day DEM₀ acting as a base for paleogeographic reconstruction was obtained from the Global
155 Bathymetric Chart of the Ocean (GEBCO) (Sandwell et al., 2002; Becker et al., 2009). The DEM for the Baltic Sea region spans from 9.5 to 31°E in longitude and from 52 to 66.5°N in latitude. The spatial resolution of the GEBCO grid is 15 arc seconds ($0.004167^\circ \times 0.004167^\circ$) and was interpolated to our Baltic Sea grid ($0.01^\circ \times 0.01^\circ$). Maintaining original resolution is unnecessary as the eustatic and isostatic components were characterized by significantly lower resolution. Such transformation had negligible influence on the quality of the generated maps, in parallel allowing to boost the map
160 generation speed and save storage space.

3.2. Eustatic data (EC)

For generation of the regional sea level curve, a dataset by Waelbroeck et al. (2002) was used as a base. However, adjustment to the regional paleogeographic setting is needed. The Baltic water level curve followed the Waelbroeck et al. (2002) data for the brackish-marine stages, namely from 11.7 kyr BP to 11 kyr BP (Yoldia Sea) and from 9.5 kyr BP till
165 present day (Littorina Sea), respectively (Andrén et al., 2011). Knowing that during the Ancylus Lake stage (11 to 9.5 kyr BP) the water level in the Baltic basins was generally higher than that in the open ocean, a local water level dataset of the southern Baltic region from Uścinowicz (2006) was applied to adjust the curve correspondingly. Even though the local relative sea level curves are strongly influenced by the Glacio-Isostatic Adjustment (Andrén et al., 2002, 2011; Groh et al., 2017; Rosentau et al., 2012, 2021; Harff et al., 2017), the southern Baltic region is located near the isostatically neutral
170 hinge-line between uplift in the north and subsidence in the south (Stattegger and Leszczyńska, 2023). Therefore glacio-isostatic adjustment played a minor role in estimation of the relative water level in the southern Baltic region. Such feature allowed to incorporate sea level values of the Ancylus Lake from Uścinowicz (2006) as “eustatic component” into the Eq. (2). Moreover, lake phase of the Baltic region refers to two independent water level systems, one for the Ancylus Lake and the other for the North Sea. The border between these two water bodies was set based on the paleo-catchment areas obtained
175 using “Terrain Aspect” function in the Golden Software Surfer on previously generated paleo-DEMs. In the lake phase, the water level in the Baltic basin followed the curve in Uścinowicz (2006), whereas in the North Sea it followed the curve in Waelbroeck et al. (2002). These two curves are shown in Fig.3.



180 **Figure 3:** Holocene water level curve for the Baltic region generated by combination of Waelbroeck et al. (2002) and Uścinowicz (2006).

3.3. Vertical crustal movements - Glacio-Isostatic Adjustment (GIA) including paleo-ice-thickness model

The solid Earth's response to the changing surface loads of the vanishing Pleistocene ice sheets is known as glacial isostatic adjustment (GIA). This visco-elastic response comprises an instantaneous elastic and a delayed viscous component.

185 GIA manifests in terms of deformations of the Earth's crust, changes in relative sea-level, i.e. sea level with respect to the Earth's deformable crust, and changes in gravitational potential (e.g. Peltier, 1998). The later originates from the redistribution surface masses, i.e. the melting of ice masses and the fresh water consequently added to the ocean, as well as from material in the Earth's mantle relocated as a reaction to the changing surface loads.

190 The decreased stress on the Earth's crust induced by the melting of the Laurentian Ice Sheet after last glacial maximum (LGM) about 21 kyr BP caused a crustal deformation which is still ongoing (Root et al., 2015). The crust is uplifting in regions formerly covered by ice. Crustal subsidence can be observed in regions surrounding the former ice cover known as the peripheral bulge (Steffen and Wu., 2011). This subsidence originates from the relocation of mantle material back to its original location in the Earth's interior underneath the region formerly covered by the ice (Vink et al., 2007). The crustal uplift is partly compensated by the additional water load stemming from the fresh-water influx. However, the melt
195 water is unevenly distributed over the ocean according to the changing gravitational potential caused by the varying distribution of ice masses as well as by the water masses themselves. Thus, close to the melting ice sheets, a drop in relative sea-level can be observed due to both the decreasing gravitational attraction of the ice and the uplifting crust.

200 The complex interaction between changing ice and water loads, their gravitational potential as well as the induced crustal deformations is described in a gravitational self-consistent way by the sea-level equation (e.g., Farrell and Clark, 1976; Peltier, 1998). To solve the sea-level equation and model the GIA-induced vertical crustal deformation we used the freely available software package SELEN (Spada and Stocchi, 2007). This software makes use of the ICE-5G ice load history (Peltier, 2004) to describe the spatio-temporal evolution of the ice sheets from LGM until present day at a temporal resolution of 1 kyr. A time interval of 500 years required for this study was achieved by assuming a linear trend between each millennium. Figure 4 depicts the ice thickness at LGM (21 kyr BP) according to the ICE-5G load history as
205 implemented by the SELEN software package. Cumulated crustal deformations are modelled starting from an equilibrium state at LGM. Details of the applied model set-up are provided in Groh and Harff (2023). The resultant GIA dataset was interpolated to our $0.01^\circ \times 0.01^\circ$ grid.

210

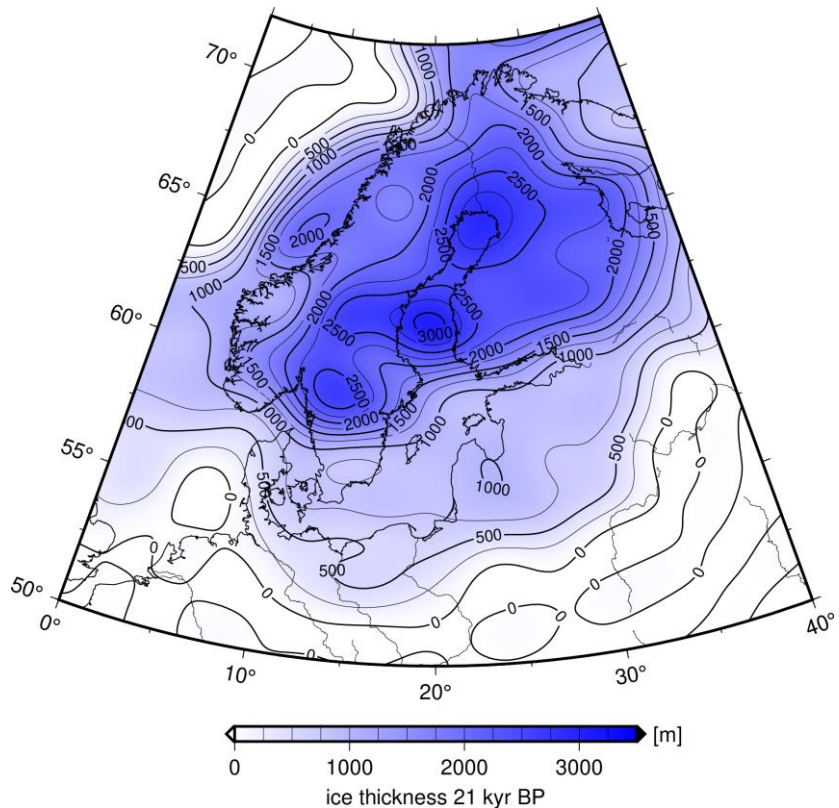


Figure 4. Present-day coastline and ice thickness at the Last Glacial Maximum (21 kyr BP) according to the ICE-5G ice load history (Peltier, 2004) as implemented by the software package of Spada and Stocchi (2007) after synthesising its spherical harmonic representation to space domain.

3.4. Sediment thickness (SED)

215 The Baltic Sea Basin is administrated by nine countries: Denmark, Germany, Poland, Sweden, Lithuania, Latvia, Estonia, Finland and Russia. Due to a fact that no joint Holocene sediment thickness database is available, it is necessary to identify and merge various existing local datasets from publicly available sources. To generate a consistent regional sediment thickness model, eight local datasets were synthesized (Fig. 5). These sub-datasets were derived by six methods of data acquisition, including digitalization of isopach maps, recalculation of thickness from seismic reflector depth maps ,
 220 interpretation of 2-D seismo-acoustic profiles and data interpolation with ordinary kriging, interpolation with ordinary kriging of point data from sediment cores, extrapolation using co-kriging, and extrapolation using convolutional neural network. All sub-datasets were produced at $0.01^\circ \times 0.01^\circ$ resolution.

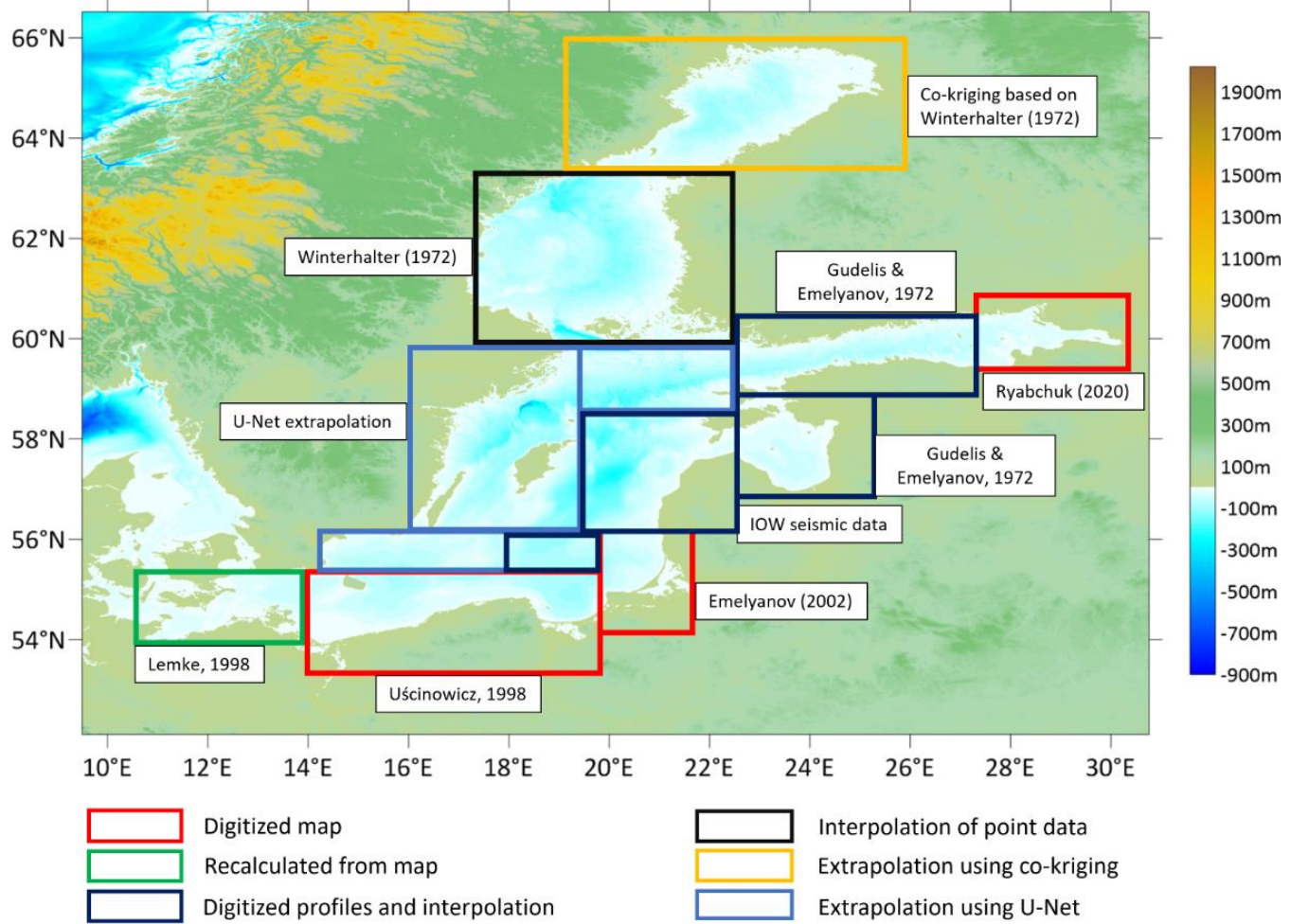


Figure 5: Map marking different types of data sources with generation of sediment thickness sub-datasets by digitalization of published Holocene isopach maps (red), recalculation of thickness from seismic reflector depth maps (green), digitalization of profiles and data interpolation (dark blue), interpolation of point data (black) as well as extrapolation using co-kriging (yellow) and convolutional neural network (bright blue).

3.4.1. Southern Baltic region

The southern Baltic Sea area consists of German, Danish, Polish, Russian (Kaliningrad area) and Lithuanian coastal waters and is characterized by well-documented Holocene sediment thickness data with satisfactory quality. The sediment thickness model was generated as a result of merging three local-scale datasets. The German and Danish parts were covered by data derived from Lemke (1998). The depth of the top layer of glacial till corresponds to the Pleistocene basement, which was subtracted from the present-day DEM in order to estimate the Holocene sediment thickness. The

235 sediment thickness data for the Polish waters was provided by Uścinowicz (1998), whereas data for the Russian (Kalininograd area) and Lithuanian territories were retrieved from Emelyanov (2002). Due to slight differences in thickness values on the border between these two datasets, the values at the grid junction were averaged.

3.4.2. Central Baltic region

240 The central Baltic (Bornholm Basin, East Gotland Basin, and its surroundings) Holocene thickness grids were retrieved from 2-D seismo-acoustic profiles collected by Leibniz-Institute for Baltic Sea Research Warnemünde (IOW), Germany (courtesy of Dr. Peter Feldens). In total 240 seismic lines, collected between 2005 and 2009, were investigated. The Holocene basement corresponds mostly to the top of glacial till (Late Pleistocene age, non-stratified seismic facies). The top of glacial till is a well-visible seismic reflector on most profiles, whereas the boundary between the BIL and the Yoldia Sea is difficult to discern in some profiles. Since the BIL belongs to the late Pleistocene, the thickness for the Holocene sediment may be slightly overestimated in these profiles. Maximum local thickness of BIL sediments up to 7 m is found in 245 the deepest parts of the basins and diminishes towards the shallower areas according to Christiansen et al. (2002). Therefore, our estimated thickness of the Holocene sediment might be overestimated by ~20% in the deepest part of the basins, with the uncertainty decreasing towards the shallower areas. The seismic reflector corresponding to the pre-Holocene basement was exported as depth data points (= shot points), transformed from the two-way travel time to metric units assuming a sound velocity in sediment of 1600 m/s, and further interpolated using ordinary kriging with nugget effect (Wackernagel and 250 Wackernagel, 2003). The obtained basement subsurface depth data were subtracted from the present-day DEM to generate the Holocene sediment thickness model.

3.4.3. Eastern Baltic region

255 Holocene sediment thickness data of the Gulf of Riga as well as of the Gulf of Finland was generated based on profiles provided by Gudelis and Emelyanov (1976). Sub-datasets consisted of 5 N-S oriented profiles connecting edges of Gulf of Finland and 6 profiles (4 NW-SE, 1 N-S, 1 W-E oriented) across the Gulf of Riga. The reflector corresponding to the top of glacial till was digitized and exported as point data, and then interpolated using ordinary kriging with nugget effect and subtracted from the present-day DEM. Thickness data covering the Russian part of the Gulf of Finland were derived from a digitized sediment thickness map by Ryabchuk et al. (2020).

3.4.4. Northern Baltic region

260 Holocene thickness data in the northern Baltic region is scarce because the area is undersampled. A mean post-glacial thickness dataset by Winterhalter (1972) consisting of 72 polygons ($0.5^\circ \times 0.5^\circ$ resolution) located in the Bothnia Sea served as a base for interpolation. The central point of each polygon was exported as a data point and then interpolated using ordinary kriging. To fill the data gap in the severely undersampled northern part of the Bothnian Bay, data points of thickness from Winterhalter (1972) were used for extrapolation by co-kriging (Goovaerts, 1998; Myers 1982, 1984). The co-
265 kriging extrapolation method is commonly used in geoscience for areas where correlated measurements of multivariate variables are available (Belkhiri et al. 2020; Leenaers et al. 2020; Konomi et al., 2023). In the northern Baltic region, a two-dimensional variable consisting of a GIA-corrected paleo-bathymetry and thickness of Holocene sediments was used. Parameters of the corresponding semi-co-variogram were determined using those grid nodes where data of both variables were available. These parameters allowed a co-kriging estimation of thickness data northward for undersampled areas.

270 **3.4.5. Filling of data gaps**

Machine learning was applied to fill the remaining gaps in the Holocene sediment thickness data. The areas with data gaps mainly include the central western part of the Baltic Sea (see Fig. 5). A convolutional neural network (CNN), namely a *U-Net* (Ronneberger et al., 2015) was build using *PyTorch* (Paszke et al., 2019). *U-Nets* have been proven to be a robust and versatile tool for image and data analysis (Zhang et al., 2018; Liu et al., 2020) and are superior to pixel-based methods such as
275 random forest (Boston et al., 2022). In this study four variables, namely the paleo-land-surface morphology, the median grain size of surface sediments and longitude and latitude values were used to predict sediment thickness. The reason for adding the latter two variables is their relationship with the GIA (Fig.4). The available data were randomly cut into 420 squares of 32×32 pixels size, excluding the Gulf of Finland and the Gulf of Bothnia. The reason for excluding the two regions is because they differ substantially in geological, tectonic, and depositional environment from the central, south, and southwest parts of the
280 Baltic Sea (Harff et al., 2017). This helps to reduce the error in the predictions. In the 420 sub-datasets, 80% were used for model training and 20% for assessment of the model prediction. The input of the *U-Net* has the shape (32, 32, 4) and the output shape is (32, 32). The first layer consists of a double convolutional block performing 3×3 convolution with 64 output channels, padding, batch normalization and ReLU activation. The training was performed with 100 epochs and the mean squared error (MSE) was calculated as the loss function (*torch.nn.MSELoss*). Re-running the model with different random initializations and
285 dropout yields different model results with the same general pattern but some local differences in sediment thickness. The result with the smallest value of MSE (6.1 m^2) was chosen (Fig.6). This corresponds to an average deviation from the validation to the measured data of 5.8%.

3.4.6. Integration of sub-datasets

Each local Holocene thickness sub-dataset was integrated to one consistent regional grid with resolution of $0.01^\circ \times 0.01^\circ$. Small spatial gaps between the sub-datasets the thickness were linearly interpolated. In case of dataset not covering the coastline, the solution proposed by Miluch et al. (2021) was used by setting equidistant pinpoints characterized by 0-thickness value along the coastlines and included into the dataset. Such solution allowed to linearly extrapolate the thickness data between the grid points and the coastline to completely close the remaining data gaps. It is worth to note that the synthesized sediment thickness dataset does not cover the present-day land parts except for barrier islands that have been developed during the Holocene. Details on the data source, density as well as interpolation and extrapolation techniques are listed in Table 1.

Table 1: List of sub-datasets of Holocene sediment thickness with information on gridding techniques as well as primary data type and density.

Area	Sub-dataset	Gridding technique	Primary data type and data density
SW Baltic region	Lemke (1998)	Recalculation and digitalization of map	Isopach map generated based on shallow seismic profiles (no. >300) and sediment cores (no. >250)
S Baltic region	Uścinowicz (1998)	Digitalization of map	Isopach map based on shallow seismic profiles and sediment cores
SE Baltic region	Emelyanov (2002)	Digitalization of map	Isopach map based on shallow seismic profiles and sediment cores
Gulf of Riga	Gudelis and Emelyanov (1972)	Digitalization of cross-sections, ordinary kriging	6 seismic lines
Gulf of Finland	Gudelis and Emelyanov (1972)	Digitalization of cross-sections, ordinary kriging	5 seismic lines
East Gotland Basin	IOW seismic data	Seismic data interpretation, ordinary kriging	240 seismic lines
E Gulf of Finland	Ryabchuk (2020)	Digitalization of map	Isopach map based on shallow seismic profiles and sediment cores

S Bothnian Bay	Winterhalter (1972)	Ordinary kriging	72 data points
N Bothnian Bay	Winterhalter (1972)	Extrapolation with co-kriging	Not available
W Baltic, N Baltic Proper	Extrapolation to undersampled areas	Extrapolation with U-Net	Not available

300

3.5. Sediment budget analysis

Generation of thickness map allows to perform sediment budget analysis that helps identify sediment sources, sinks and transport pathways. The grid was transformed from the geographic coordinate system to UTM projection to conduct volume calculation. Applied volume calculation algorithms include the trapezoidal rule, the Simpson's rule and the

305 Simpson's 3/8 rule (Atkinson, 1989). Each method approximates different 3-D connection shapes between the data points, which slightly influences the calculated volume. Results from the algorithms were compared to assess the uncertainty.

Sediment mass calculation requires information of sediment bulk density that is related to sediment particle density and porosity. Surface sediment porosity was calculated based on the present-day sediment grain size map of the Baltic Sea derived from the project DYNAS (Dynamics of Natural and Anthropogenic Sedimentation) (Bobertz et al., 2009; Harff et

310 al., 2011) and application of the empirical formula from Endler et al. (2015) to link porosity to the median grain size.

Knowing that compaction rates of sandy and silty sediments is neglectable at a thickness scale of meter (Schmedemann et al., 2008), constant vertical porosity depending on the local grain size was assumed for the Holocene deposit. Pores volume was subtracted from the general volume. Knowing that Baltic Sea sediments are mainly clastic (Anthony et al., 2009), quartz density = 2.65 g/cm³ was used as the particle density. With the gridded data of porosity and sediment thickness and a

315 constant particle density, the overall mass of the Baltic Sea Holocene sediments as well as annual rate of deposition averaged over the period are estimated.

3.6. Generation of paleogeographic maps

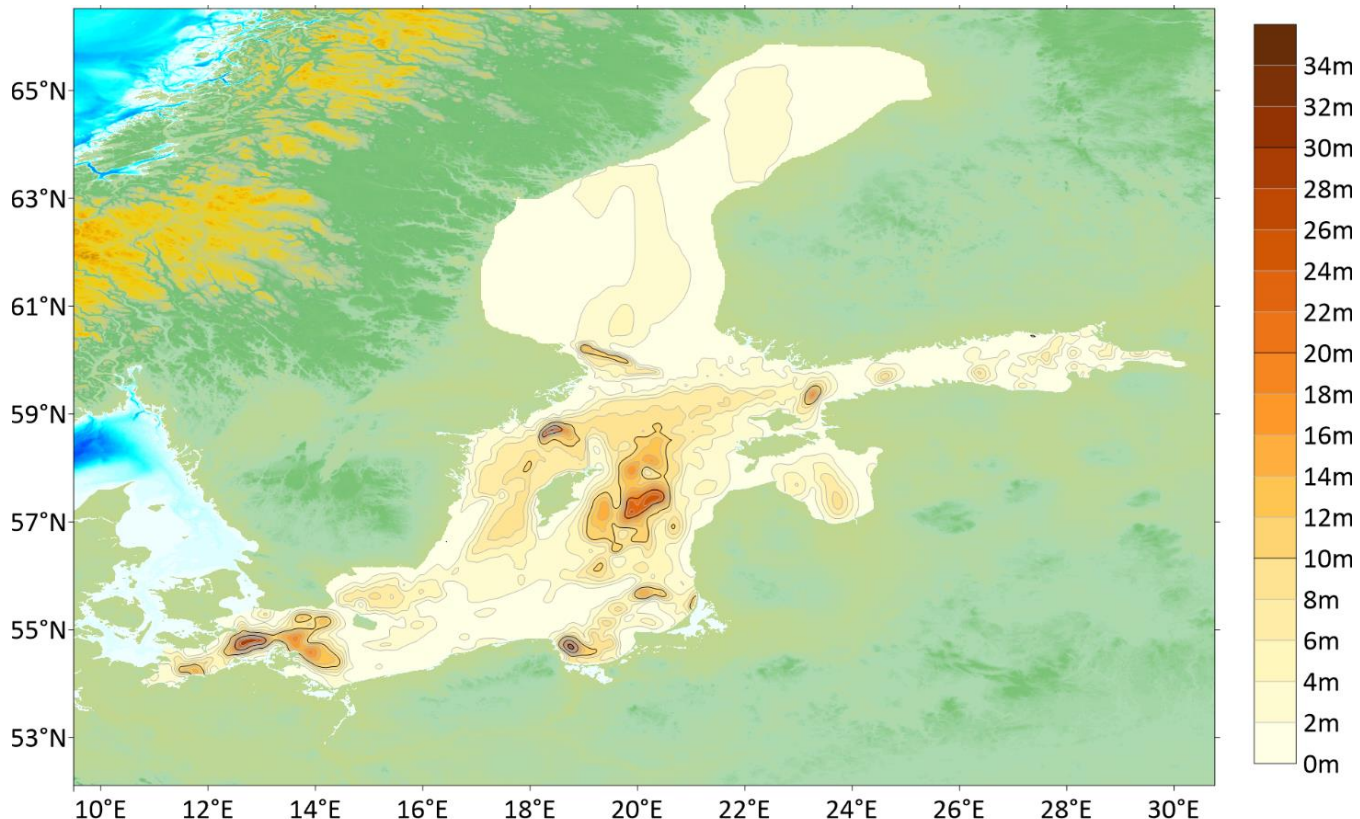
Having all the needed components described in Equation (1) and (2), namely the eustatic sea level change, the spatial distribution of the GIA and the sediment depositional thickness, the present-day DEM₀ was transformed into a set of

320 paleo DEMs for the Baltic Sea, mimicking the paleogeographic evolution of the region with fine spatio-temporal resolution (Supplementary Materials). The thickness of sediment deposition for each time slice ($\Delta t = 500$ yrs) was subtracted from the total Holocene thickness assuming constant sediment accumulation rate.

4. Results

4.1. Holocene sediment thickness map

325 Integration of 8 local-scale sediment thickness datasets with extrapolation methods allowed to generate a regional Holocene sediment thickness map (Fig. 6). Several sites characterized by high sediment thickness were identified in southern and central parts of the Baltic Sea, corresponding to depressions of sub-basins including the Arkona Basin, the Bornholm Basin as well as the Eastern and Western Gotland Basins. Maximum deposition thickness reaches up to 36 m in the Arkona Basin and the Eastern Gotland Basin. Although regions of enhanced sediment accumulation are usually located in deeper 330 basins, some shallower coastal areas also host locally confined deposits with thickness larger than 20 m. These include the central sections of the Gulf of Finland, the Gulf of Riga (both coupled with local bathymetry, as reported by Jakobsson et al. (2019)) as well as the Gdańsk Basin. The thick Holocene deposit in the Gdańsk Basin is related to the formation of the Hel Peninsula that is driven by alongshore sediment transport (Uścinowicz, 2022). In contrast to the southern Baltic Sea, the 335 Holocene sediment thickness in the northern Baltic Sea is relatively thin and mostly within 6 m. Such feature may be related to the glacio-isostatic uplift resulting in a continuous reduction of accommodation space in the Bothnian Sea and the Bothnian Bay (Varela, 2015). The characteristics of seabed substrate of the northern Baltic Sea confirm the presence of glacial clay, hard bottom complexes and bedrocks covered by a thin layer of Holocene sand and gravel (Kaskela et al., 2012).



340 **Figure 6:** Regional Holocene thickness model derived from synthesis of 8 local sub-datasets and application of 3 extrapolation methods (Table 1).

4.2. Sediment budget

Sediment volume calculated using the trapezoidal rule, the Simpson's rule and the Simpson's 3/8 rule, respectively provided nearly identical results (<0.001% difference, see Supplementary Materials). The calculated total volume of Holocene sediment is $1.372 \times 10^{12} \text{ m}^3$ in bulk. Subtracting the sediment porosity yields a zero-porosity sediment volume of $5.07 \times 10^{11} \text{ m}^3$, corresponding to a total Holocene sediment mass of $1.34 \times 10^{12} \text{ t}$ and an annual sediment accumulation of $1.15 \times 10^8 \text{ t yr}^{-1}$ (averaged over 11700 yrs) in the Baltic Sea.

Potential errors in the estimation may originate from several sources, including porosity, grain density, vertical compaction and unclear boundary between late Pleistocene and early Holocene in the seismic profiles. The standard deviation σ of porosity is ~ 0.15 according to the sediment samples analyzed by Endler et al. (2015). Applying the mean $\pm \sigma$ in the porosity data as the upper and lower estimates respectively indicates a range between $0.82 \times 10^{12} \text{ t}$ and $1.87 \times 10^{12} \text{ t}$ in the total sediment mass. Although the Holocene deposits mainly consist of silt and sand, the deeper basins (e.g. Arkona,

Bornholm and Gotland) are covered by a layer of mixture of organic matter (up to 16%) and clay (Leipe et al., 2011) that is subjected to the impact of vertical compaction. The thickness of such layer can extend to several meters in the deep basins 355 (Andrén et al., 2000; Ponomarenko, 2023). Assuming that the average thickness of this layer is 4 m (as indicated in a majority of sediment cores) in the basins, neglection of the vertical compaction results in an overestimation of the porosity by $\sim 10\%$ according to Schmedemann et al. (2008), corresponding to an underestimation of sediment mass of $\sim 0.055 \times 10^{12}$ t, which accounts for $\sim 4\%$ of the estimated mean total budget (1.34×10^{12} t). As described in section 3.4.2, unclear boundary 360 between late Pleistocene and early Holocene sediment in the seismic profiles across the deep basins (e.g. the Gotland basin) may lead to overestimation of the Holocene sediment thickness by $\sim 20\%$ in the deepest part of the basins. The overestimation decreases toward shallower areas. A uniform overestimation of the deposition thickness in the basins by 20% corresponds to a sediment budget of 1.1×10^{11} t, which is $\sim 8\%$ of the estimated mean total budget (1.34×10^{12} t). In summary, 365 considering the uncertainties related to the major identified sources mentioned above in the estimation yields a range of the total Holocene sediment budget between 0.81×10^{12} t and 1.82×10^{12} t, corresponding to annual sediment accumulation rate between 0.69×10^8 t yr $^{-1}$ and 1.56×10^8 t yr $^{-1}$.

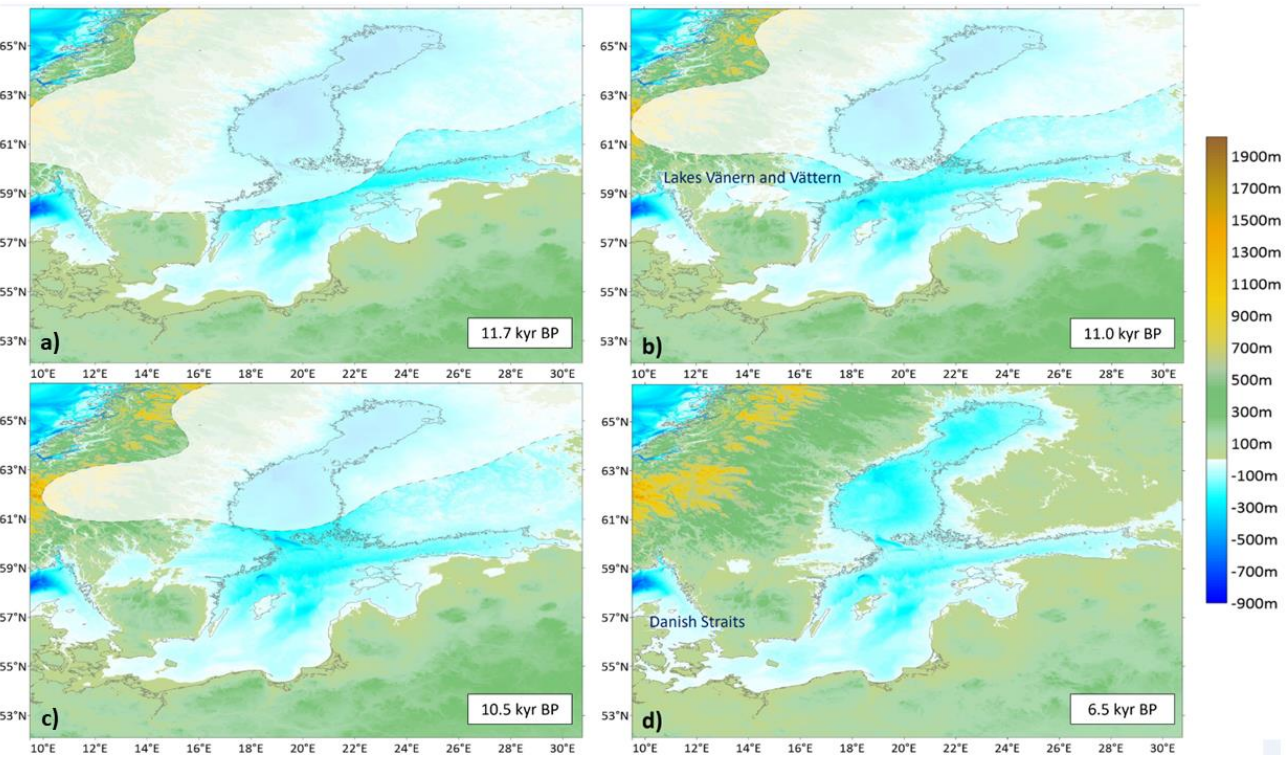
4.3. Paleogeographic maps

A set of paleogeographic maps with a time interval of 500 years reflecting the evolution of the Baltic Sea region during the Holocene is provided in the Supplementary Materials, with maps for several periods marking a critical transition in the sea level change shown in Fig. 7. To evaluate the paleogeographic maps, a reference is made to the widely used maps 370 derived from proxy data interpretation (Fig. 1) produced by Andrén et al. (2011).

At ~ 11.7 kyr BP, a transition from the BIL to the Yoldia Sea stage occurred. At that time, a large part of the north of today's Baltic Sea basin was covered by the glaciers of the Fennoscandian Ice Sheet (FIS). The water level of the Baltic 375 Ice Reservoir was dammed up to 25 m above the present-day sea level (Andrén et al., 2011) before the lake water made its way through the Central Swedish Depression in the southern border of the FIS and flowed into the paleo-North Sea basin in a drainage event in today's Kattegat (Fig. 7a). Rising sea level outpacing the moderate uplift of the mainland in the immediate vicinity of south of the ice margin in the Central Swedish Depression sustained a free exchange of water through 380 a gate between the Baltic Sea and the North Sea for several centuries that marks a brackish-marine phase called the Yoldia Sea Stage (11.7 – 11.0 kyr BP). Both maps, the paleo-DEM shown in Fig. 7b and that of Andrén et al. (2011) shown in Fig. 1b confirm the existence of such a gate. The maps clearly show the course of the inherent BIL drainage in the lowlands of the Central Swedish Depression through lakes Vänern and Vättern. This drainage course was near the margin of the FIS. According to Patton et al. (2017), Shaw et al. (2006) and Stokes et al., (2015), the continental ice front is not considered as a stable line but rather consists of multiple glacial-fluvial channels between large ice blocks. The central Swedish lowlands were characterized by such an environment, enabling the water flow between the Baltic Sea and the North Sea during the Yoldia Sea period (Fig. 7a and 7b). During the Yoldia Sea stage (Fig. 7b) the sea level in the open North Sea and the water

385 level in the Baltic Sea basin converged and lasted until ~11.0 kyr BP. As the ice front continued to retreat northwards, the increasing uplift of Scandinavia outpaced the eustatic sea level rise and closed the gate in the central Swedish lowlands. The Baltic Sea consequently reverted to a freshwater environment, namely the Ancylus Lake, fed primarily by meltwater from the remnants of the FIS, which still covered the highlands of Scandinavia. The increasing flow of meltwater into the Ancylus Basin led to a rise in the lake level (so-called “Ancylus Transgression”) reaching a peak at ~10.5 kyr BP and a subsequent
390 drainage of the lake water into the paleo-North Sea (Fig. 7c). Different from the drainage through the central Swedish lowlands in the later stage of the BIL, the freshwater outflow in the late stage of the Ancylus Lake moved to the south due to the increasing glacio-isostatic uplift of Scandinavia and took place through the area of today's western Baltic Sea, namely the Danish Straights. In the generation of the maps, we distinguished the water levels between the Lake Ancylus and the open North Sea from 11.0 to 9.5 kyr BP according to Uścinowicz (2006), which are shown in Fig. 3.

395 At ~9.5 kyr BP, the one-way drainage from the Baltic Sea (Lake Ancylus) to the North Sea ceased due to a rise of the eustatic sea level which caught up with the water level in the Lake Ancylus (Harff et al. 2017), and the Littorina transgression enabled a free exchange between the Baltic Sea and the open North Sea again (Fig. 7d). Since then, the global sea-level change has dominated the hydrographic regime in the Baltic Sea. Glacio-isostatic movements of the region lead to persistent transgression in the south and regression in the north of the Baltic Sea (Harff et al. 2017). The paleogeographic
400 setting at 6.5 kyr BP is illustrated by the map shown in Fig. 7d. A comparison with the map generated by Andrén et al. (2011) based on proxy data shown in Fig. 1c shows a general agreement in the reconnection of the Baltic Sea basin to the open North Sea and verifies our model result.



405 **Figure 7:** Reconstructed paleogeographic maps representing different stages of the Baltic Sea. Four exemplary maps are depicted here for comparison with the paleogeographic maps generated by Andrén et al. (2011). a) Baltic Ice Lake/Yoldia Sea transition at 11.7 kyr BP; b) Yoldia Sea (end of the brackish phase) at 11.0 kyr BP; c) Akyllus Lake (maximum transgression) at 10.5 kyr BP; d) Littorina Sea (most saline phase) at 6.5 kyr BP. The present-day coastline is depicted by the gray line and the ice cover is indicated by the transparent mask.

410 **4.4 Validation of the paleogeographic reconstruction**

An interplay between eustasy and spatially varied rates of isostatic rebound is mirrored in various local RSL curves. Reconstructed curves for all subareas of the Baltic Sea Basin gathered by Rosentau et al. (2021) allowed to locally assess our numerically modelled paleogeographic maps. All station data located along the eastern (Berglund, 2012; Hansson et al., 2018) and the northern Swedish coast (Linden et al., 2006) as well as the Finnish coast (Glückert, 1976; Saarnisto, 1981; 415 Mietinen, 2003) suggest a decreasing RSL since 11.7 kyr BP whereas stations in the southern Baltic coast mirror a consistent rising RSL that slows down and stabilizes after 6.0 kyr BP (Lampe et al., 2004, 2011; Gelumbauskaite, 2009; Uścinowicz et al., 2011). Stations along the Latvian and Estonian coast (Grudzińska et al., 2013, 2014; Lougas, and Tomek, 2013; Berzins et al., 2016) infer a general decreasing RSL interrupted by the Akyllus transgression. The reported local RSL curves show discrepancy with our model results mainly for the initial stage between 11.7- 10 kyr BP and afterward a general agreement 420 (Fig.8). The opposite patterns of the RSL change between the northern and southern coasts gradually converge towards the

central Baltic area where eustatic and isostatic components neutralize each other. This is seen at the stations in Latvia and Blekinge which show a relatively flat RSL curve with small-scale variations (Damusyte, 2011; Rosentau et al., 2013; Habicht et al., 2017). Such relatively stable RSL is reproduced in our results, albeit with discrepancy in the period between 11.7 and 10 kyr BP for the Blekinge station and between 11 and 8 kyr BP for the Latvia station (Fig.8). A general agreement 425 between our modelled RSL and local RSL curves compiled by Rosentau et al. (2021) as well as an agreement in the connection/disconnection between the open North Sea and the Baltic basin described in the previous section validate the approach applied in this study.

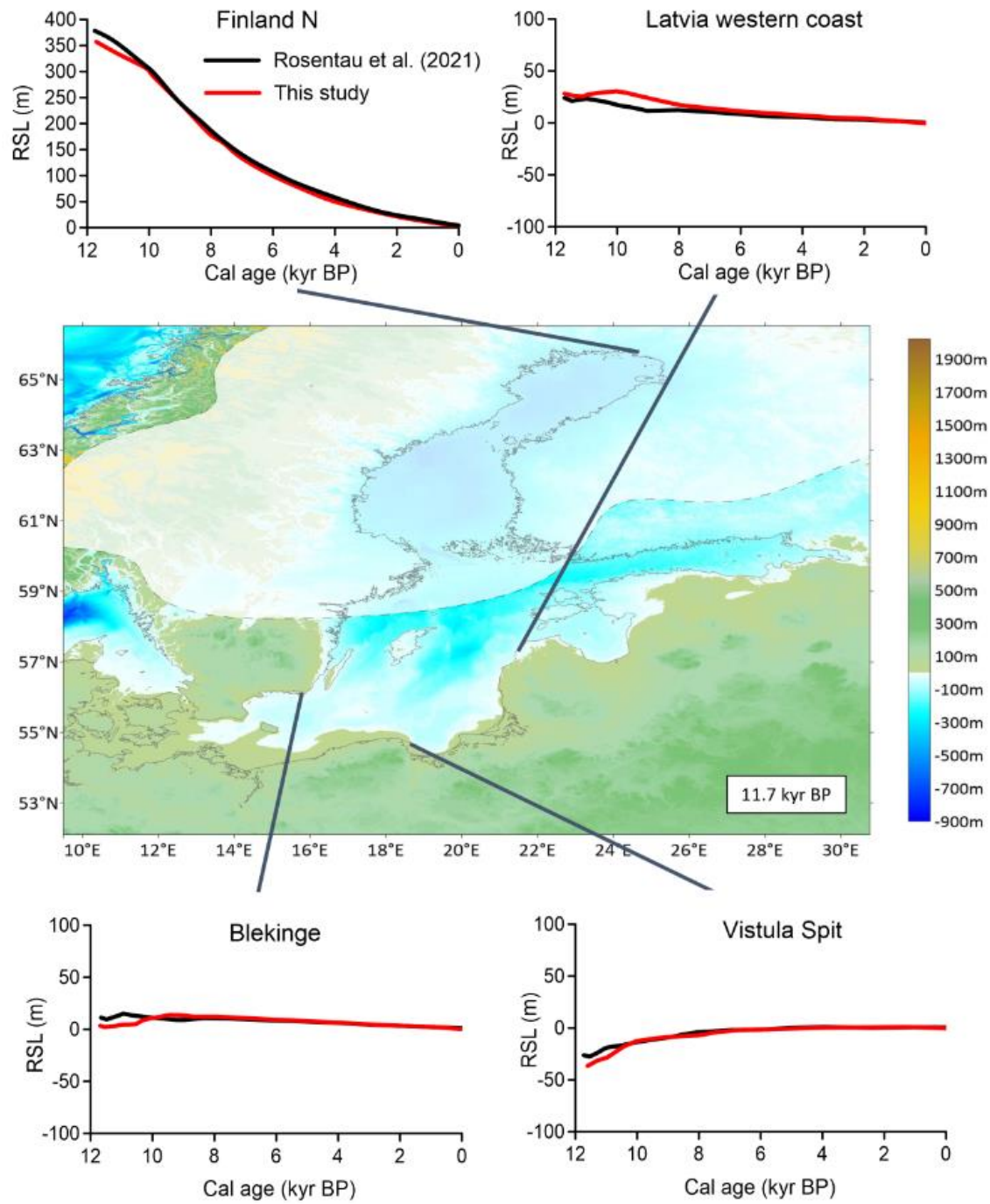


Figure 8. Comparison of our modelled RSL (red curves) and local RSL curves (black curves) derived from the ICE-5G

430 model with 120 km lithosphere thickness by Rosentau et al. (2021).

5. Discussion

5.1. Comparison with existing reconstructions

The maps generated in this study are further assessed by comparison with existing local reconstructions. A

435 comparison of RSL curves between those by Rosentau et al. (2021) and our results shows a general agreement except for the early Holocene period, as described in the previous section. In three stations, namely Finland N, Blekinge and Vistula Spit, our results show a lower RSL at 11.7 kyr BP than those in Rosentau et al. (2021) adopting 120 km lithosphere thickness (Fig. 8). It should be noted that there exist remarkable differences in the reconstructed local RSLs for the early Holocene period among the scenarios adopting different lithosphere thickness values as shown in Rosentau et al (2021). As pointed out 440 by Rosentau et al. (2021), the reconstructed curves using global ICE-5G and ICE-6G_C ice histories overestimate the RSL and fail to capture a mid-Holocene high-stand (~7.5-6.5 kyr BP) inferred from the proxy data in the transitional area. This overestimation seems to originate from an overestimation of ice loading in the ICE-5G and especially in the ICE-6G_C models. Our modelled curves lie in the lower limit of the RSLs in Rosentau et al. (2021), and therefore may provide results closer to proxy data.

445 We also compared our modelled paleo-DEM with the maps from Andrén et al. (2011) in a qualitative manner and identified a general consistency between the two sets of maps in the location of the gates between the Baltic basin and the open North Sea as well as the timing of their closing and opening (section 4.3). Nevertheless, some local scale differences are also seen between our results and the maps of Andrén et al. (2011), e.g. on the morphology of the Bornholm Island and the Gotland Island. In the map of Andrén et al. (2011), both islands are emerged already in 11.7 kyr BP. By contrast, our 450 map shows that the Island of Bornholm is still connected to the mainland and the Gotland Island is largely submerged at that time. The shape of the coastline remains similar, however a higher RSL in the southern part and lower RSL in the western and eastern parts of the Baltic Sea are seen in Andrén et al. (2011) compared to our result. Such difference may be attributed to that the map of Andrén et al. (2011) represents still the late stage of BIL when the water level was higher in the Baltic basin than the North Sea, whereas our result corresponds to the beginning of the post-drainage phase when the water level of 455 these two seas converged. For the maximum of *Ancylus* transgression at 10.5 kyr BP, a state when the North Sea and the Baltic Sea are disconnected, a difference in the coastline location of the northern Baltic region between the two maps is seen. The difference indicates a lower RSL leading to emerging of the west Estonian archipelago and Finland in the map of Andrén et al. (2011) compared to our result. Noteworthy is that even though the difference in the coastline position seems to be huge, the difference in the elevation is relatively small (mostly within 10 m), suggesting that the land-sea transition in this 460 part is highly sensitive to the change of RSL and therefore slight modification of isostatic or eustatic components may have significant influence in the coastline position. Our reconstructed morphology of the Littorina Sea at 6.5 kyr BP is characterized by an open connection between the Baltic Sea and the North Sea through the Danish Straits, which persists until today. In the reconstruction by Andrén et al. (2011), the Baltic-North Sea connection at 6.5 kyr BP exists only via the

Great Belt, whereas all three straits are already opened in our result at that time. The timing of events such as opening of
465 straits varies between reconstructions. Some local-scale topographic structures such as straits may not be well resolved in regional reconstructions due to insufficient spatial resolution or data coverage. Similar to earlier scenarios, the RSL in the northern and central parts of the Baltic Sea is generally lower in the map of Andrén et al. (2011) compared to our result.

An earlier effort in mapping Holocene sediment thickness in the Baltic Sea has been made by Jakobson
470 et al. (2007). The mapping was through assembling information from available sediment distribution maps and information retrieved from the Swedish Geological Survey's mapping archives which unfortunately do not provide an open access. The resultant map is characterized by relatively low spatial resolution and limited to the southern and central parts (without Bothnian Bay) of the Baltic Sea (Jakobson et al., 2007). A comparison
475 between our map (Figure 5) and that from Jakobson et al. (2007) shows a general agreement in the Borholm basin and along the Swedish coast near the Gotland. However, there exists a large discrepancy in the thickness value in other basins (e.g. Arkona basin, Gotland basin) between the two maps. The thickness values in Jakobson et al. (2007) for these basins are much smaller than previous published values from Lemke (1998) and Uścinowicz (1998) focusing on these local areas. Despite a likely overestimation of the Holocene sediment thickness in the deep Gotland basin as pointed out in section 3.4.2, integrated data from the difference sources within this study
480 show more consistent patterns covering both deep basins and shallow coastal areas and therefore provide a more accurate distribution of Holocene sediment thickness.

5.2. Major source and sink terms in the Holocene Baltic Sea

A comparison of the annual sediment accumulation rate averaged over the Holocene with the present day's estimation by Porz et al. (2021) suggests that they are at the same order of magnitude for the SW Baltic Sea. The Holocene-
485 averaged accumulation rate is $8.8 \pm 4.1 \times 10^6$ t yr⁻¹ in the SW Baltic Sea according to our data in this study. In the budget analysis done by Porz et al. (2021), the annual accumulation rate of fine-grained sediment in the SW Baltic Sea basins is between 5.5×10^6 and 8.2×10^6 t yr⁻¹.

Coastal erosion, namely erosion of the glacial-till cliffs, serves as the main source that contributes at least 80% of the annual deposition in the basins (Wallmann et al., 2022). Sediment supply from major central European rivers, namely
490 Oder, Vistula, Nemunas, Daugava and Neva, is on the order of 1×10^7 t yr⁻¹ (Porz et al., 2021; Pruszak et al., 2005; Lajczak and Jansson, 1993) with the largest contribution from the river Vistula ($0.16-0.4 \times 10^7$ t yr⁻¹). This indicates that the riverine sediment supply accounts for less than 10% of the total Holocene sediment budget in the Baltic Sea. Biogenic production contributes to 4-15% of the annual deposition budget (Wallmann et al., 2022; Porz et al., 2021). In addition, sediment input

from the North Sea is estimated to be on the order of 1×10^6 t yr⁻¹, contributing to 10-30% of the annual deposition in the SW
495 Baltic Sea (Porz et al., 2021). However, this input is almost negligible (accounting for ~1%) compared to the total annual accumulation rate in the Baltic Sea. Additional supply of sediment from melting of the ice cover on the Scandinavia may occur during early Holocene stages. However, such supply might also be negligible compared to the total Holocene sediment budget given that the Scandinavian mountains provide only a very small suspended sediment yield that is on the order of 1×10^5 t yr⁻¹ (Lajczak and Jansson, 1993).

500 It is worth to note that our Holocene sediment thickness map is spatially confined by the present-day Baltic Sea coast. Although Holocene sedimentation may also occur on parts of the present-day mainland especially in the northern Baltic coast when they were submerged, the deposited sediment was subjected to reworking when these parts became emerged and therefore is difficult to quantify due to lack of data. Moreover, the Holocene sediment thickness of the northern Baltic Sea and its coast is generally scarce (Fig.6), therefore omission of deposit on the mainland is considered to have minor
505 impact on the paleo-DEMs and the total Holocene sediment budget in the Baltic Sea.

5.3. Importance of integrating sediment dynamics in paleogeographic reconstructions

Depending on the regional or local setting, the individual impact of eustatic, isostatic/tectonic and sediment dynamics on geographical and morphological development of marginal seas may vary significantly. Inclusion of sediment dynamics in paleogeographic reconstruction of coastal regions and continental shelves that are fed by significant terrestrial
510 sediment input has critical influence on the location of the paleo-coastline and general morphology of the seabed. This has been demonstrated in the paleo-reconstructions of the Beibu Gulf in the northern South China Sea (Xiong et al., 2020; Zhang et al., 2020), the Pearl River delta and its estuary (Wu et al., 2010), the Mekong River delta and adjacent shelf (Wang et al., 2024), the southwestern coast of Bohai Sea (Liu et al., 2016) and the southern North Sea (Van der Molen and Van Dijck, 2000).

515 The integration of sediment dynamics is also important for understanding the evolution of large-scale sedimentary systems which are not directly fed by riverine sediment but are formed and/or shaped by sediment transport, such as barrier islands (Zhang et al., 2011a; Zhang et al., 2014; Karle et al., 2021) and mud depocenters (Porz et al., 2021). This process is especially important for evolution of the southern Baltic Sea where various barrier islands have developed since mid-Holocene when the sea level has approached a relatively stable level (Uścinowicz et al., 2011; Zhang et al., 2011b;
520 Dudzińska-Nowak, 2017). It is worth noting that although many paleogeographic reconstructions exist at local scales by considering sediment transport dynamics, our work represents the first attempt for a consistent reconstruction at a marginal sea scale. Comprehensive information of dated sediment thickness for a marginal sea such as the Baltic Sea is difficult to obtain, as most of relevant datasets are derived locally and it requires extensive effort in collection, integration, harmonization and synthesis of such datasets and filling of gaps between them. A consistent paleogeographic reconstruction
525 of a marginal sea considering not only regional processes such as eustatic sea level change and isostatic/tectonic movement

but also sediment deposition provides indispensable information on the historical development of the marginal sea especially its coast.

A future challenge towards improvement of paleogeographic reconstructions requires differentiation of sediment accumulation and erosion rates. Although sediment accumulation rate may vary throughout the Holocene, we adopted a constant rate in this study due to poor data constraint. The reported rates were mostly derived based on analysis of sparsely distributed sediment cores and it is difficult to extrapolate a few tens of point data to the entire Baltic Sea. Therefore, more measurement data is needed to provide a sound database for extrapolation. Mass-balanced reconstruction methods have been proposed for backstripping of depositional areas and backfilling of erosional areas at geological time scales (Hay et al., 1989; Feng et al., 2023). However, these are of high uncertainty for reconstructions at a millennial scale due to insufficient resolution in the seismo-acoustic profiles. An attempt to reconstruct the eroded coastal landscape in mid Holocene has been done by Zhang et al. (2014) at a local scale. The reconstruction was based on an extrapolation of the shape of present-day remnants of erodible coast by a fitted spline function using the morphology of the backland as a reference. Based on the identified major source and sink terms as well as the associated transport pathways exemplified in this study, it might also be feasible to apply the same method to reconstruct eroded coasts at a centennial-to-millennial time scale.

540 6. Conclusions

This study presents a spatially high-resolution ($0.01^\circ \times 0.01^\circ$) paleogeographic reconstruction of the Baltic Basin including the coastal evolution of the Baltic Sea for the Holocene since the end of the Baltic Ice Lake stage at 11.7 kyr BP. These data describe the surface structure of the study area, climate-induced eustatic sea level change, glacio-isostatic (GIA) vertical Earth's crust movement and the thickness of sediment deposition in the Baltic Sea basin. Local datasets of sediment thickness from open sources including existing literature and data portals with public access were compiled and complemented by numerical interpolation and extrapolation to generate a consistent regional map of Holocene sediment thickness for the entire Baltic Sea. The map shows that relatively thick Holocene sediments are deposited in the southern and central parts of the Baltic Sea, filling the sub-basins, including Arkona, Bornholm, Eastern and Western Gotland and Northern Central Basins, with a maximum thickness of up to 36 m. In addition, some shallower coastal areas in the southern 545 Baltic Sea also host localized deposits with a thickness of more than 20 m, mostly associated with alongshore sediment transport and formation of barrier islands and spits. In contrast to the southern Baltic Sea, the thickness of Holocene sediments in the northern Baltic Sea is relatively low, mostly less than 6 m. The total mass of Holocene sediment in the Baltic Sea is estimated to be between 0.81×10^{12} t and 1.82×10^{12} t, corresponding to annual sediment accumulation rate between 0.69×10^8 t yr $^{-1}$ and 1.56×10^8 t yr $^{-1}$.

555 For the first time, the paleogeographic reconstruction of the Baltic Sea for the Holocene was achieved by a combination of crustal deformation (GIA), eustatic water level change and sediment thickness considering the disconnection of paleo-North Sea and the easterly freshwater body during the Ancylus Lake stage. The model results are validated by comparison with field-based proxy data interpretation. This comparison improves the reconstruction of the hydrographic

connection between the Baltic Sea and the North Sea in the marginal zone of the former Fennoscandian Ice Sheet. Our work
560 thus represents a further step towards a consistent methodology to reconstruct the formation of marginal seas during transgression/regression cycles including not only tropic and subtropic climate zones but also polar and subpolar marginal seas impacted by the regional dynamics of ice sheets.

Acknowledgements

This study is an outcome of the project “Morphological evolution of coastal seas – past and future”

565 (<https://marginalseas.ddeworld.org/margseas-rd-research-project>) funded by the Deep-time Digital Earth program (<https://www.ddeworld.org/>). It is also supported by the Helmholtz PoF programme “The Changing Earth – Sustaining our Future” on its Topic 4: Coastal zones at a time of global change.

Authors contribution

570 Wenyan Zhang designed and supervised the study. Jakub Miluch collected, digitized, and processed sediment data and eustatic sea level curve of the study area. He also generated the paleogeographic maps by numerical modeling supervised by Jan Harff. Andreas Groh provided the data and GIA scenarios used for paleogeographic modeling and contributed related text descriptions. Peter Arlinghaus applied the convolutional neural network to fill the data gaps in the sediment thickness. Celine Denker assisted in collection, digitization, and generation of the sediment thickness map. Jakub Miluch and Wenyan
575 Zhang wrote the original manuscript. All authors have contributed to manuscript revision. We thank for Peter Feldens for providing seismic data and Labiqah Zahid for her assistance in collection, digitization, and generation of the sediment thickness map.

Data availability

580 Publicly available datasets were analyzed in this study. Present-day digital elevation model of the Baltic Sea is derived from GEBCO 2023 Grid (doi:10.5285/f98b053b-0cbc-6c23-e053-6c86abc0af7b). Seismic profiles in the Gotland Basin were kindly provided by Dr. Peter Feldens from the Leibniz Institute for Baltic Sea Research (IOW). Gridded Holocene sediment thickness data produced in this study can be found at the Mendeley Data with doi: 10.17632/k45mff2ccy.1

585 Competing interests

The contact author has declared that none of the authors has any competing interests.

References

590 Andrén, E., Andrén, T., Sohlenius, G.: The Holocene history of the southwestern Baltic Sea as reflected in a sediment core from the Bornholm Basin. *Boreas*, 29(3), 233-250, <https://doi.org/10.1111/j.1502-3885.2000.tb00981.x>, 2000.

Andrén, T., Lindeberg, G., Andrén, E.: Evidence of the final drainage of the Baltic Ice Lake and the brackish phase of the Yoldia Sea in glacialvarves from the Baltic Sea. *Boreas* 31, 226–238, <https://doi.org/10.1111/j.1502-3885.2002.tb01069.x>, 2002.

595 Andrén, T., Björck, S., Andrén, E., Conley, D., Zillén, L., Anjar, J.: The Development of the Baltic Sea Basin During the Last 130 ka. In: Harff, J., Björck, S., Hoth, P. (eds) *The Baltic Sea Basin. Central and Eastern European Development Studies (CEEDES)*. Springer, Berlin, Heidelberg. https://doi.org/10.1007/978-3-642-17220-5_4, 2011.

Anthony, J.W., Bideaux, R.A., Bladh, K.W., Nichols, M.C.: *Handbook of Mineralogy III (Halides, Hydroxides, Oxides)*. Mineralogical Society of America, Chantilly, VA, United States, 2009.

600 Allen, P.A., Allen, J.R.: *Basin Analysis – Principles and Applications*. Blackwell Publishing, Oxford, pp. 1–549., 2008.

Atkinson, K.E.: *An Introduction to Numerical Analysis*, second ed. John Wiley Sons, New York, United States, 1989.

Becker, J. J., Sandwell, D. T., Smith, W. H. F., Braud, J., Binder, B., Depner, J., Fabre, D., Factor, J., Ingalls, S., Kim, S-H., Ladner, R., Marks, K., Nelson, S., Pharaoh, A., Trimmer, R., Von Rosenberg, J., Wallace, G., Weatherall, P.: Global Bathymetry and Elevation Data at 30 Arc Seconds Resolution: SRTM30_PLUS. *Marine Geodesy*, 32(4), 355–371. <https://doi.org/10.1080/01490410903297766>, 2009.

605 Belkhiri, L., Tiri, A., Mouni, L.: Spatial distribution of the groundwater quality using kriging and Co-kriging interpolations. *Groundwater for Sustainable Development*, 11, 100473, 2020.

Berglund, M.: Early Holocene in Gästrikland, east central Sweden: shore displacement and isostatic recovery. *Boreas*, 41(2), 263–276, <https://doi.org/10.1111/j.1502-3885.2011.00228.x>, 2012.

610 Berra, F., Jadoul, F., Anelli, A.: Environmental control on the end of the Dolomia Principale/Hauptdolomit depositional system in the central Alps: coupling sea-level and climate changes. *Palaeogeography, Palaeoclimatology, Palaeoecology*, 290(1-4), 138–150, <https://doi.org/10.1016/j.palaeo.2009.06.037>, 2010.

Bērziņš, V., Lübke, H., Berga, L., Cericā, A., Kalniņa, L., Meadows, J., Muižniece, S., Paegle, S., Rudzīte, M., Zagorska, I.: Recurrent Mesolithic–Neolithic occupation at Sise (western Latvia) and shoreline displacement in the Baltic Sea Basin. *The Holocene*, 26(8), 1319–1325. <https://doi.org/10.1177/0959683616638434>, 2016.

615 Björck, S.: A review of the history of the Baltic Sea, 13.0–8.0 ka BP. *Quaternary international*, 27, 19–40, [https://doi.org/10.1016/1040-6182\(94\)00057-C](https://doi.org/10.1016/1040-6182(94)00057-C), 1995.

Björck, S.: The late Quaternary development of the Baltic Sea basin. In *Assessment of climate change for the Baltic Sea Basin* (pp. 398–407). Springer, 2008.

620 Bola, A., Kayode, J.S.: An evaluation of digital elevation modeling in GIS and Cartography, *Geo-spatial Information Science*, 17:2, 139–144, <https://doi.org/10.1080/10095020.2013.772808>, 2014.

Bobertz, B., Harff, J., Bohling, B.: Parameterisation of clastic sediments including benthic structures. *Journal of Marine Systems*, 75 (3-4), pp. 371–381. <https://doi.org/10.1016/j.jmarsys.2007.06.010>, 2009.

Boston, T., Van Dijk, A., Larraondo, P.R., Thackway, R.: Comparing CNNs and Random Forests for Landsat Image Segmentation Trained on a Large Proxy Land Cover Dataset. *Remote Sens.*, 14, 3396. <https://doi.org/10.3390/rs14143396>, 2022.

625 Covington, J.H., P., Kennelly, P.: Paleotopographic influences of the Cretaceous/Tertiary angular unconformity on uranium mineralization in the Shirley Basin, Wyoming, *Journal of Maps*, 14:2, 589–596, <https://doi.org/10.1080/17445647.2018.1512014>, 2018.

Christiansen, C., Kunzendorf, H., Emeis, K.-C., Endler, R., Struck, U., Neumann, T., Sivkov, V., Temporal and spatial sedimentation rate variabilities in the eastern Gotland Basin, the Baltic Sea. *Boreas*, Vol. 31, pp. 65–74, <https://doi.org/10.1111/j.1502-3885.2002.tb01056.x>, 2002.

630 Damušytė, A.: Post-glacial geological history of the Lithuanian coastal area, Doctoral Dissertation, Physical Sciences, Geology, Vilnius. 2011.

Dudzińska-Nowak, J.: Morphodynamic processes of the Swina Gate coastal zone development (southern Baltic Sea). *Coastline Changes of the Baltic Sea from South to East: Past and Future Projection*, 219–255, 2017.

Einsele, G.: Event deposits: the role of sediment supply and relative sea-level changes—overview. *Sedimentary Geology*, 104(1-4), 11–37, [https://doi.org/10.1016/0037-0738\(95\)00118-2](https://doi.org/10.1016/0037-0738(95)00118-2), 1996.

635 Emelyanov E.: Geology of the Gdańsk Basin, Russian Academy of Sciences, Atlantic Branch of P. P. Shirshov Institute of Oceanology, Yantarny skaz, Russian Federation, 2002.

640 Endler, M., Endler, R., Bobertz, B., Leipe, T., Arz, H.W.: Linkage between acoustic parameters and seabed sediment properties in the south-western Baltic Sea. *Geo-Marine Letters*, 35, 145-160, <https://doi.org/10.1007/s00367-015-0397-3>, 2015.

Farrell, W., Clark, J.: On Postglacial Sea Level. *Geophys. J. Int.* 46, 647—667, <https://doi.org/10.1111/j.1365-246X.1976.tb01252.x>, 1976.

645 Feng, B., He, Y., Li, H., Li, T., Du, X., Huang, X., Zhou, X.: Paleogeographic reconstruction of an ancient source-to-sink system in a lacustrine basin from the Paleogene Shahejie formation in the Miao xibei area (Bohai Bay basin, east China). *Front. Earth Sci.* 11:1247723. doi: 10.3389/feart.2023.1247723, 2023.

Gale, A. S., Hardenbol, J., Hathway, B., Kennedy, W. J., Young, J. R., Phansalkar, V.: Global correlation of Cenomanian (Upper Cretaceous) sequences: Evidence for Milankovitch control on sea level. *Geology*, 30(4), 291-294, [https://doi.org/10.1130/0091-7613\(2002\)030%3C0291:GCOCUC%3E2.0.CO;2](https://doi.org/10.1130/0091-7613(2002)030%3C0291:GCOCUC%3E2.0.CO;2), 2002.

650 GEBCO Compilation Group (2023) GEBCO 2023 Grid (doi:10.5285/f98b053b-0cbc-6c23-e053-6c86abc0af7b)

Gelumbauskaitė, L. Ž.: Character of sea level changes in the subsiding south-eastern Baltic Sea during Late Quaternary. *Baltica*, 22(1), 23-36, 2009.

Glückert, G.: Post-glacial shore-level displacement of the Baltic in SW Finland. *Ann. Acad. Sci. Fenn., Ser. A III* 118, 1976.

655 Golden Software Surfer User's Guide (p. 446–448). Available on-line https://gis.fns.uniba.sk/vyuka/DTM_ako_suast_GIS/Kriging/2/Surfer_8_Guide.pdf (last accessed 16th December 2023).

Gonet, T. and Gonet, K.: Alternative Approach to Evaluating Interpolation Methods of Small and Imbalanced Data Sets, *Geomatics and Environmental Engineering* 11(3), 49-65, <http://dx.doi.org/10.7494/geom.2017.11.3.49>, 2017.

660 Goovaerts, P.: Ordinary cokriging revisited. *Mathematical Geology*, 30, 21-42, 1998.

Groh, A., Harff, J.: Relative sea-level changes induced by glacial isostatic adjustment and sediment loads in the Beibu Gulf, South China Sea. *Oceanologia* 65(1), 249—259. <https://doi.org/10.1016/j.oceano.2022.09.001>, 2023.

Grudzinska, I., Saarse, L., Vassiljev, J., Heinsalu, A.: Mid-and late-Holocene shoreline changes along the southern coast of the Gulf of Finland. *Bulletin of the Geological Society of Finland*, 85, 2013.

665 Grudzinska, I., Saarse, L., Vassiljev, J., Heinsalu, A.: Biostratigraphy, shoreline changes and origin of the Limnea Sea lagoons in northern Estonia: the case study of Lake Harku. *Baltica*, 27(1), <https://doi.org/10.5200/baltica.2014.27.02>, 2014.

Grund, S., Geiger, J.: Sedimentologic modelling of the Ap-13 hydrocarbon reservoir. *Central European Geology*, 54/4, pp. 327–344, <https://doi.org/10.1556/CEuGeol.54.2011.4.2>, 2011.

670 Groh, A., Richter, A., Dietrich, R.: Recent Baltic Sea Level Changes Induced by Past and Present Ice Masses. In: Harff, J., Furmańczyk, K., von Storch, H. (eds) *Coastline Changes of the Baltic Sea from South to East*. Coastal Research Library, vol 19. Springer, Cham. https://doi.org/10.1007/978-3-319-49894-2_4, 2017.

Gudelis, V., Emelyanov, E. (eds.): *Geology of the Baltic Sea*, Mokslas Publishers, 1976.

Habicht, H. L., Rosentau, A., Jõeleht, A., Heinsalu, A., Kriiska, A., Kohv, M., Hang, T., Aunap, R.: GIS-based multiproxy coastline reconstruction of the eastern Gulf of Riga, Baltic Sea, during the Stone Age. *Boreas*, 46(1), 83-99, <https://doi.org/10.1111/bor.12157>, 2017.

675 Hall, A., van Boeckel, M.: Origin of the Baltic Sea basin by Pleistocene glacial erosion. *Gff*, 142(3), 237-252, <https://doi.org/10.1080/11035897.2020.1781246>, 2020.

Hansson, A., Nilsson, B., Sjöström, A., Björck, S., Holmgren, S., Linderson, H., Magnell, O., Rundgren, M., Hammarlund, D., A submerged Mesolithic lagoonal landscape in the Baltic Sea, south-eastern Sweden—Early Holocene environmental reconstruction and shore-level displacement based on a multiproxy approach. *Quaternary International*, 463, 110-123, <https://doi.org/10.1016/j.quaint.2016.07.059>, 2018.

680 Harff, J.; Lemke, W.; Lampe, R.; Lüth, F.; Lübke, R.; Meyer, M.; Tauber, F.; Schmölcke, U.: The Baltic Sea Coast – a Model of Interrelations between Geosphere, Climate and Anthroposphere. – In: Harff, J.; Hay, W.W.; Tetzlaff, D. (eds.): *Coastline Change – Interrelation of Climate and Geological Processes*. – The Geological Society of America, Spec. Pap. 426, pp. 133-142, 2007.

685 Harff, J., Endler, R., Emelyanov, E., Kotov, S., Leipe, T., Moros, M., Olea, R.A., Tomczak, M., Witkowski, A.: Late Quaternary Climate Variations reflected in Baltic Sea Sediments.- in. Harff, J., Björck, S., Hoth, P. (eds.). *The Baltic Sea Basin*.- Springer. Berlin et al., p. 99-132, 2011.

690 Harff, J., Deng, J., Dudzinska-Nowak, J., Fröhle, P., Groh, A., Hünicke, B., Soomere, T., Zhang, W.: What Determines the Change of Coastlines in the Baltic Sea? 2017, in: Harff, J., Furmanczyk, K., von Storch, H. (eds) 2017. *Coastline Changes of the Baltic Sea from South to East - Past and Future Projection* Coastal Research Library, vol 19. Springer, Heidelberg, pp 15-35, https://doi.org/10.1007/978-3-319-49894-2_4, 2017.

695 Hay, W.W., Shaw, C.A., Wold, C.N.: Mass-balanced paleogeographic reconstructions. *Geol Rundsch* 78, 207–242. <https://doi.org/10.1007/BF01988362>, 1989.

700 Heinsalu, A., Veski, S.: The history of the Yoldia Sea in Northern Estonia: palaeoenvironmental conditions and climatic oscillations. *Geological Quarterly*, 51, 295-306, 2007.

705 Hulskamp, R., Luijendijk, A., van Maren, B. et al. Global distribution and dynamics of muddy coasts. *Nat Commun* 14, 8259, <https://doi.org/10.1038/s41467-023-43819-6>, 2013.

710 Jakobsson, M., Björck, S., Alm, G., Andrén, T., Lindeberg, G., Svensson, N. O.: Reconstructing the Younger Dryas ice dammed lake in the Baltic Basin: Bathymetry, area and volume. *Global and Planetary Change*, 57(3-4), 355-370, <https://doi.org/10.1016/j.gloplacha.2007.01.006>, 2007.

Jakobsson, M., Stranne, C., O'Regan, M., Greenwood, S. L., Gustafsson, B., Humborg, C., and Weidner, E.: Bathymetric properties of the Baltic Sea, *Ocean Sci.*, 15, 905–924, <https://doi.org/10.5194/os-15-905-2019>, 2019.

715 Karle M, Bungenstock F, Wehrmann A.: Holocene coastal landscape development in response to rising sea level in the Central Wadden Sea coastal region. *Netherlands Journal of Geosciences* 100, e12. <https://doi.org/10.1017/njg.2021.10>, 2021.

Kaskela, A. M., Kotilainen, A. T., Al-Hamdani, Z., Leth, J. O., Reker, J.: Seabed geomorphic features in a glaciated shelf of the Baltic Sea. *Estuarine, Coastal and Shelf Science*, 100, 150-161., <https://doi.org/10.1016/j.ecss.2012.01.008>, 2012.

720 Konomi, B. A., Kang, E. L., Almomani, A., Hobbs, J.: Bayesian Latent Variable Co-kriging Model in Remote Sensing for Quality Flagged Observations. *Journal of Agricultural, Biological and Environmental Statistics*, 1-19, 2023.

Lambeck, K., Purcell, A., Zhao, J., Svensson, N. O.: The Scandinavian ice sheet: from MIS 4 to the end of the last glacial maximum. *Boreas*, 39(2), 410-435, <https://doi.org/10.1111/j.1502-3885.2010.00140.x>, 2010.

725 Lampe, R., Janke, W.: The Holocene sea level rise in the Southern Baltic as reflected in coastal peat sequences. *Polish geological institute Special papers*, 11, 19-29, 2004.

730 Lampe, R., Endtmann, E., Janke, W., Meyer, H.: Relative sea-level development and isostasy along the NE German Baltic Sea coast during the past 9 ka. *E&G Quaternary Science Journal*, 59(1/2), 3-20, <https://doi.org/10.3285/eg.59.1-2.01>, 2011.

Leenaers, H., Burrough, P. A., Okx, J. P.: Efficient mapping of heavy metal pollution on floodplains by co-kriging from elevation data. In *Three Dimensional Applications in GIS* (pp. 37-50). CRC Press, 2020.

735 Leipe, T., Tauber, F., Vallius, H., Virtasalo, J., Uścinowicz, S., Kowalski, N., Hille, S., Lindgren, S., Myllyvirta, T.: Particulate organic carbon (POC) in surface sediments of the Baltic Sea. *Geo-Mar Lett* 31, 175–188, <https://doi.org/10.1007/s00367-010-0223-x>, 2011.

Lemke, W.: *Sedimentation und paläogeographische Entwicklung im westlichen Ostseeraum (Mecklenburger Bucht bis Arkonabecken) vom Ende der Weichselvereisung bis zur Litorinatransgression*. Institut für Ostseeforschung Warnemünde, 1998.

Lemke, W., Jensen, J. B., Bennike, O., Endler, R., Witkowski, A., Kuijpers, A.: Hydrographic thresholds in the western Baltic Sea: Late Quaternary geology and the Dana River concept. *Marine Geology*, 176(1-4), 191-201, [https://doi.org/10.1016/S0025-3227\(01\)00152-9](https://doi.org/10.1016/S0025-3227(01)00152-9), 2001.

740 Libina, N.V., Nikiforov, S.L.: Digital Elevation Models of the Bottom in the Operational Oceanography System. *Oceanology* 60, 854–860, <https://doi.org/10.1134/S0001437020050124>, 2020.

Lindén, M., Möller, P. E. R., Björck, S., Sandgren, P. E. R., Holocene shore displacement and deglaciation chronology in Norrbotten, Sweden. *Boreas*, 35(1), 1-22, <https://doi.org/10.1111/j.1502-3885.2006.tb01109.x>, 2006.

Liu, L., Xing, F., Li, Y., Han, Y., Wang, Z., Zhi, X., Wang, G., Feng, L., Yang, B., Lei, Y., Fan, Z., Du, W.: Study of the geostatistical grid maths operation method of quantifying water movement in soil layers of a cotton field, *Irrig and Drain*, 69:1146–1156, <https://doi.org/10.1002/ird.2513>, 2020.

Liu, N., He, T., Tian, Y., Wu, B., Gao, J., Xu, Z.: Common azimuth seismic data fault analysis using residual U-Net. *Interpretation*. 8. 1-41. <https://doi.org/10.1190/int-2019-0173.1>, 2020.

740 Liu, Y., Huang, H., Qi, Y., Liu, X., Yang, X.: Holocene coastal morphologies and shoreline reconstruction for the southwestern coast of the Bohai Sea, China. *Quaternary Research*, 86(2):144-161.
<https://doi.org/10.1016/j.yqres.2016.06.002>, 2016.

745 Lõugas, L., Tomek, T.: Marginal effect at the coastal area of Tallinn Bay: The marine, terrestrial and avian fauna as a source of subsistence during the Late Neolithic. *Man, his time, artefacts, and paces. Collection of articles dedicated to Richard Indreko*. Muinasaja teadus, 19, 463-485, 2013.

750 Luijendijk, A., Hagenaars, G., Ranasinghe, R., Baart, F., Donchyts, G., Aarninkhof, S.: The State of the World's Beaches. *Sci Rep* 8, 6641, <https://doi.org/10.1038/s41598-018-24630-6>, 2018.

755 Lajczak, A., Jansson, M.B.: Suspended Sediment Yield in the Baltic Drainage Basin. *Hydrology Research* 24 (1): 31–52. doi: <https://doi.org/10.2166/nh.1993.0003>, 1993.

760 Maystrenko, Y., Bayer, U., Brink, H. J., Littke, R.: The Central European Basin System – an Overview. In: Littke, R., Bayer, U., Gajewski, D., Nelskamp, S. (eds) *Dynamics of Complex Intracontinental Basins*. Springer, Berlin, Heidelberg. https://doi.org/10.1007/978-3-540-85085-4_2, 2008.

765 Matthäus, W., Franck, H.: Characteristics of major Baltic inflows—a statistical analysis. *Continental Shelf Research*, 12(12), 1375-1400, [https://doi.org/10.1016/0278-4343\(92\)90060-W](https://doi.org/10.1016/0278-4343(92)90060-W), 1992.

770 Mentaschi, L., Vousdoukas, M. I., Pekel, J. F., Voukouvalas, E., Feyen, L.: Global long-term observations of coastal erosion and accretion. *Sci Rep* 8, 12876, <https://doi.org/10.1038/s41598-018-30904-w>, 2018.

775 Miettinen, A. I.: Relative sea level changes in the eastern part of the Gulf of Finland during the last 8000 years, 2003.

Miluch, J., Osadczuk, A., Feldens, P., Harff, J., Maciąg, Ł., Chen, H., 2021.: Seismic profiling-based investigation of geometry and sedimentary architecture of the late Pleistocene delta in the Beibu Gulf, SW of Hainan Island. *J. Asian Earth Sci.* 205, 104611. <https://doi.org/10.1016/j.jseas.2020.104611>, 2021.

780 Miluch J., Maciąg Ł., Osadczuk A., Harff J., Jiang T., Chen H., Borówka R.K., McCartney, K.: Multivariate geostatistical modeling of seismic data: Case study of the Late Pleistocene paleodelta architecture (SW off-shore Hainan Island, South China Sea), *Marine and Petroleum Geology, Marine and Petroleum Geology* 136, 105467, <https://doi.org/10.1016/j.marpetgeo.2021.105467>, 2022.

785 Myers, D. E.: Matrix formulation of co-kriging. *Journal of the International Association for Mathematical Geology*, 14, 249-257, 1982.

790 Myers, D. E.: Co-kriging—new developments. In *Geostatistics for Natural Resources Characterization: Part 1* (pp. 295-305). Dordrecht: Springer Netherlands, 1984.

Neumann, B., Vafeidis, A. T., Zimmermann, J., Nicholls, R. J.: 2015. Future Coastal Population Growth and Exposure to Sea-Level Rise and Coastal Flooding—A Global Assessment. *PLoS ONE* 10, e0118571, <https://doi.org/10.1371/journal.pone.0118571>, 2015.

795 Paszke, A., Gross, S., Massa, F., Lerer, A., Bradbury, J., Chanan, G., Killeen, T., Lin, Z., Gimelshein, N., Antiga, L., Desmaison, A., Kopf, A., Yang, E., DeVito, Z., Raison, M., Tejani, A., Chilamkurthy, S., Steiner, B., Fang, L., Bai, J., Chintala, S.: PyTorch: An Imperative Style, High-Performance Deep Learning Library. In *Advances in Neural Information Processing Systems* 32, edited by H. Wallach, H. Larochelle, A. Beygelzimer, F. d'Alché-Buc, E. Fox, and R. Garnett, Pp. 8024–8035. Curran Associates, Inc. Publisher's Version, 2019.

800 Patton, H., Hubbard, A., Andreassen, K., Auriac, A., Whitehouse, P. L., Stroeven, A. P., Shackleton, C., Winsborrow, M., Heyman, J., Hall, A. M.: Deglaciation of the Eurasian ice sheet complex. *Quaternary Science Reviews*, 169, 148-172, <https://doi.org/10.1016/j.quascirev.2017.05.019>, 2017.

805 Peltier, W., Postglacial variations in the level of the sea: Implications for climate dynamics and solid-earth geophysics. *Rev. Geophys.* 36, 603–689. <https://doi.org/10.1029/98RG02638>, 1998.

810 Peltier, W. R.: Global sea level rise and glacial isostatic adjustment. *Global and planetary change*, 20(2-3), 93-123, [https://doi.org/10.1016/S0921-8181\(98\)00066-6](https://doi.org/10.1016/S0921-8181(98)00066-6), 1999.

815 Peltier, W.: Global glacial isostasy and the surface of the ice-age Earth: the ICE-5G (VM2) model and GRACE. *Annu. Rev. Earth Pl. Sc.* 32, 111—149. <https://doi.org/10.1146/annurev.earth.32.082503.144359>, 2004.

820 Peltier, W. R.: Postglacial coastal evolution: ice–ocean–solid Earth interactions in a period of rapid climate change, [https://doi.org/10.1130/2007.2426\(02\)](https://doi.org/10.1130/2007.2426(02)), 2007.

825 Ponomarenko, E.: Holocene palaeoenvironment of the central Baltic Sea based on sediment records from the Gotland Basin, *Regional Studies in Marine Science*, Volume 63, 102992, <https://doi.org/10.1016/j.rsma.2023.102992>, 2023.

Porz, L., Zhang, W., Schrum, C.: Density-driven bottom currents control development of muddy basins in the southwestern Baltic Sea. *Marine Geology*, Volume 438, 106523, <https://doi.org/10.1016/j.margeo.2021.106523>, 2021.

790 Pruszak, Z., van Ninh, P., Szmytkiewicz, M., Manh Hung, N., Ostrowski, R.: Hydrology and morphology of two river mouth regions (temperate Vistula Delta and subtropical Red River Delta), *Oceanologia*, 47 (3), 365–385, 2005.

Razas, M.A., Hassan, A., Khan, M.U., Emach, M.Z., Saki, S.A.: A critical comparison of interpolation techniques for digital terrain modelling in mining. *Journal of the Southern African Institute of Mining and Metallurgy*, 123(2), 53-62. <https://dx.doi.org/10.17159/2411-9717/2271/2023>, 2023.

795 Ronneberger, O., Fischer, P., Brox, T U-Net: Convolutional Networks for Biomedical Image Segmentation. *Medical Image Computing and Computer-Assisted Intervention (MICCAI)*, Springer, LNCS, Vol.9351: 234-241, 2015.

Root, B. C., van der Wal, W., Novák, P., Ebbing, J., Vermeersen, L. L. A.: Glacial isostatic adjustment in the static gravity field of Fennoscandia. *Journal of Geophysical Research: Solid Earth*, 120(1), 503-518, <https://doi.org/10.1002/2014JB011508>, 2015.

800 Rosentau, A., Harff, J., Oja, T., Meyer, M.: Postglacial rebound and relative sea level changes in the Baltic Sea since the Litorina transgression, *Baltica* 25 (2), 113-120, <https://doi.org/10.5200/baltica.2012.25.11>, 2012.

Rosentau, A., Muru, M., Kriiska, A., Subetto, D. A., Vassiljev, J., Hang, T., Gerasimov, D., Nordqvist, K., Ludikova, A., Lõugas, L., Raig, H., Kihno, K., Aunap, R., Letyka, N.: Stone Age settlement and Holocene shore displacement in the Narva-Luga Klint Bay area, eastern Gulf of Finland. *Boreas*, 42, 912–931, <https://doi.org/10.1111/bor.12004>, 2013.

805 Rosentau, A., Bennike, O., Uścinowicz, S., Miotk-Szpijanowicz, G.: The Baltic Sea Basin. Submerged landscapes of the European continental shelf: quaternary paleoenvironments, 103-133, <https://doi.org/10.1002/9781118927823.ch5>, 2017.

Rosentau, A., Kleemann, V., Bennike, O., Steffen, H., Wehr, J., Latinović, M., Bagge, M., Ojala, A., Berglund, M., Becher, G. P., et al.: A Holocene relative sea-level database for the Baltic Sea, *Quaternary Science Reviews*, 266, 107 071, <https://doi.org/10.1016/j.quascirev.2021.107071>, 2021.

810 Ryabchuk, D.V., Sergeev, A.Y., Prishchepenko, D.V., Zhamoida, V.A., Elkina, D.V., Piskarev, A.L., Bashirova, L.D., Ponomarenko, E.P., Budanov, L.M., Grigoriev, A.G., Evdokimenko, A.V.: Impact of climate change on sedimentation processes in the eastern Gulf of Finland during the Middle to Late Holocene. *Boreas* 50, 381-403. <https://doi.org/10.1111/bor.12500>, 2020.

Saarnisto, M.: Holocene emergence history and stratigraphy in the area north of the Gulf of Bothnia. *Suomalainen tiedeakatemia*, 1981.

815 Sandwell, D.T., Gille, S.T., Smith, W.H.F., eds., *Bathymetry from Space: Oceanography, Geophysics, and Climate*, Geoscience Professional Services, Bethesda, Maryland, 24pp., 2002.

Schmedemann, N., Schafmeister, M. T., Hoffmann, G.: Numeric de-compaction of Holocene sediments. *Polish Geological Institute Special Papers*, 23, 87-94, 2008.

820 Shaw, J., Piper, D. J. W., Fader, G. B. J., King, E. L., Todd, B. J., Bell, T., Batterson, M.J., Liverman, D. G. E.: A conceptual model of the deglaciation of Atlantic Canada. *Quaternary Science Reviews*, 25(17-18), 2059-2081. <https://doi.org/10.1016/j.quascirev.2006.03.002>, 2006.

Sohlenius, G., Emeis, K. C., Andrén, E., Andrén, T., Kohly, A. Development of anoxia during the Holocene fresh–brackish water transition in the Baltic Sea. *Marine Geology*, 177(3-4), 221-242, [https://doi.org/10.1016/S0025-3227\(01\)00174-8](https://doi.org/10.1016/S0025-3227(01)00174-8), 2001.

825 Spada, G., Stocchi, P.:SELEN: A Fortran 90 program for solving the “sea-level equation”. *Comput. Geosci.* 33, 538—562. <https://doi.org/10.1016/j.cageo.2006.08.006>, 2007.

Spada, G., Melini, D., Galassi, G., Colleoni, F.: Modeling sea level changes and geodetic variations by glacial isostasy: the improved SELEN code. *arXiv preprint arXiv:1212.5061*, <https://doi.org/10.48550/arXiv.1212.5061>, 2012.

830 Stattegger, K., Leszczyńska, K.: Rapid sea-level rise during the first phase of the Litorina transgression in the western Baltic Sea, *Oceanologia*, 65 (1), 202-210, <https://doi.org/10.1016/j.oceano.2022.05.001>, 2023.

Steffen, H., Wu, P. Glacial isostatic adjustment in Fennoscandia—a review of data and modeling. *Journal of geodynamics*, 52(3-4), 169-204, <https://doi.org/10.1016/j.jog.2011.03.002>, 2011.

835 Stokes, C. R., Tarasov, L., Blomdin, R., Cronin, T. M., Fisher, T. G., Gyllencreutz, R., Hätterstand, C., Heyman, J., Hindmarsh, R. C. A., Hughes, A. L. C., Jakobsson, M., Kirchner, N., Livingstonen, S. J., Margold, M., Murton, J. B., Noormets, R., Peltier, W. R., Piper, D. J. W., Preusser, F., Renssen, H., Roberts, D. H., Rocher, D. M.,

840 Saint-Ange, F., Stroven, A. P. Teller, J. T.: On the reconstruction of palaeo-ice sheets: recent advances and future challenges. *Quaternary Science Reviews* 125, 15–49., <https://doi.org/10.1016/j.quascirev.2015.07.016>, 2015.

Sturt, F., Garrow, D., Bradley, S.: New models of North West European Holocene paleogeography and inundation. *Journal of Archaeological Science* 40 (11), 3963-3976, <https://doi.org/10.1016/j.jas.2013.05.023>, 2013.

Uehara, K., J. D. Scourse, K. J. Horsburgh, K. Lambeck, and A. P. Purcell: Tidal evolution of the northwest European shelf seas from the Last Glacial Maximum to the present, *J. Geophys. Res.*, 111, C09025, doi:[10.1029/2006JC003531](https://doi.org/10.1029/2006JC003531), 2006.

Uścinowicz, S.: Geological Atlas of the Southern Baltic – Holocene thickness, Polish Geological Institute, 1998.

Uścinowicz, S.: A relative sea-level curve for the Polish Southern Baltic Sea, *Quaternary International*, 145–146, 86-105, <https://doi.org/10.1016/j.quaint.2005.07.007>, 2006.

Uścinowicz, S.: The Baltic Sea continental shelf. In Chiocci, F. L, Chivas, A. R (eds.) *Continental Shelves of the World: Their Evolution During the Last Glacio-Eustatic Cycle*. Geological Society Memoir, 41, 69-89, <https://doi.org/10.1144/m41.7>, 2014.

Uścinowicz, S., Miotk-Szpigajnowicz, G., Krąpiec, M., Witak, M., Harff, J., Lübke, H., Tauber, F.: Drowned forests in the Gulf of Gdańsk (Southern Baltic) as an indicator of the Holocene shoreline changes. *The Baltic Sea Basin*, 219-231, 2011.

Uścinowicz, S.: Hel Peninsula—geological structure and history. Assessing the Baltic Sea Earth System, 4th Baltic Earth Conference, Jastarnia, Poland, 30 May – 3 June 2022.

Van der Molen, J., and Van Dijck, B.: The evolution of the Dutch and Belgian coasts and the role of sand supply from the North Sea. *Glob. Planet. Chang.* 27 (1-4), 223-244. 2000.

855 Varela, A. N.: Tectonic control of accommodation space and sediment supply within the Mata Amarilla Formation (lower Upper Cretaceous) Patagonia, Argentina. *Sedimentology*, 62(3), 867-896, <https://doi.org/10.1111/sed.12164>, 2015.

Vink, A., Steffen, H., Reinhardt, L., Kaufmann, G.: Holocene relative sea-level change, isostatic subsidence and the radial viscosity structure of the mantle of northwest Europe (Belgium, the Netherlands, Germany, southern North Sea). *Quaternary Science Reviews*, 26(25-28), 3249-3275, <https://doi.org/10.1016/j.quascirev.2007.07.014>, 2007.

Völt, A.: Relative sea level changes and regional tectonic evolution of seven coastal areas in NW Greece since the mid-Holocene. *Quaternary Science Reviews*, 26(7-8), 894-919, <https://doi.org/10.1016/j.quascirev.2007.01.004>, 2007.

Wackernagel, H., Wackernagel, H.: Ordinary kriging. Multivariate geostatistics: an introduction with applications, 79-88, 2003.

860 Waelbroeck, C., Labeyrie, L., Michel, E., Duplessy, J.C., McManus, J.F., Lambeck, K., Balbon, E., Labracherie, M.: Sea-level and deep water temperature changes derived from benthic foraminifera isotopic records. *Quat. Sci. Rev.* 21, 295–305. [https://doi.org/10.1016/S0277-3791\(01\)00101-9](https://doi.org/10.1016/S0277-3791(01)00101-9), 2002.

Wallmann, K., Diesing, M., Scholz, F., Rehder, G., Dale, A.W., Fuhr, M. Suess, E.: Erosion of carbonate-bearing sedimentary rocks may close the alkalinity budget of the Baltic Sea and support atmospheric CO₂ uptake in coastal seas. *Front. Mar. Sci.* 9:968069. doi: 10.3389/fmars.2022.968069, 2022.

870 Wang, X., Zhang, W., Xie, X., Chen, H., and Chen, B.: Holocene sedimentary distribution and morphological characteristics reworked by East Asian monsoon dynamics in the Mekong River shelf, South Vietnam. *Estuarine, Coastal and Shelf Science*, Vol 302, 108784, <https://doi.org/10.1016/j.ecss.2024.108784>, 2024.

Watts, A. B.: Tectonic subsidence, flexure and global changes of sea level. *Nature*, 297(5866), 469-474, 1982.

875 Weisse, R., Dailidienė, I., Hünicke, B., Kahma, K., Madsen, K., Omstedt, A., Parnell, K., Schöne, T., Soomere, T., Zhang, W., Zorita, E. (2021): Sea level dynamics and coastal erosion in the Baltic Sea region. *Earth Syst. Dynam.*, 12, 871–898, <https://doi.org/10.5194/esd-12-871-2021>, 2021.

Winterhalter, B.: On the geology of the Bothnian Sea, an epeiric sea that has undergone Pleistocene glaciation, *Geological Survey of Finland Bulletin* 258, Geologinen Tutkimuslaitos, Otaniemi, Finland, 1972.

880 Wu, C.Y., Wei X., Ren, J., Bao, Y., He, Z.G., Lei, Y.P., Shi, H.Y., Zhang, W.: Morphodynamics of the rock-bound outlets of the Pearl River estuary, South China – A preliminary study, *Journal of Marine Systems*, 82(1), 17- 27, <https://doi.org/10.1016/j.jmarsys.2010.02.002>, 2010.

Wulff, F., Stigebrandt, A., Rahm, L.: Nutrient dynamics of the Baltic Sea. *Ambio*, 126-133, 1990.

Xiong, P., Dudzińska-Nowak, J., Harff, J., Xie, X., Zhang, W., Chen, H., Jiang, T., Chen, H., Miluch, J., Feldens, P., 885 Maciąg, Ł., Osadczuk, A., Meng, Q., Zorita, E.: Modeling paleogeographic scenarios of the last glacial cycle as a base

for source-to-sink studies: an example from the northwestern shelf of the South China Sea. *J. Asian Earth Sci.* 203, 104542. <https://doi.org/10.1016/j.jseaes.2020.104542>, 2020.

Yang, S.L., Xu, K.H., Milliman, J.D., Yang, H.F., Wu, C.S.: Decline of Yangtze River sediment discharge: impact from natural and anthropogenic changes. *Sci. Rep.* 5, 12581. <https://doi.org/10.1038/srep12581>, 2014.

890 Yao, Y., Harff, J., Meyer, M., Zhan, W.: Reconstruction of paleocoastlines for the northwestern south China sea since the last glacial maximum. *Sci. China Earth Sci.* 52, 1127–1136. <https://doi.org/10.1007/s11430-009-0098-8>, 2009.

Yilmaz, H.M.: The effect of interpolation methods in surface definition: an experimental study, *Earth Surf. Process. Landforms* 32, 1346–1361, <https://doi.org/10.1002/esp.1473>, 2007.

895 Zhang, P., Ke, Y., Zhang, Z., Wang, M., Li, P. Zhang, S. Urban Land Use and Land Cover Classification Using Novel Deep Learning Models Based on High Spatial Resolution Satellite Imagery. *Sensors*, 18, 3717. <https://doi.org/10.3390/s18113717>, 2018.

Zhang, W., Arlinghaus, P.: Climate, Coast, and Morphology. In: *Oxford Research Encyclopedia of Climate Science*. Oxford University Press, <https://doi.org/10.1093/acrefore/9780190228620.013.814>, 2022.

900 Zhang, W., Xiong, P., Meng, Q., Dudzińska-Nowak, J., Chen, H., Zhang, H., Zhou, F., Miluch, J., Harff, J.: Morphogenesis of a late Pleistocene delta off the southwestern Hainan Island unraveled by numerical modeling. *J. Asian Earth Sci.* 195, 104351. <https://doi.org/10.1016/j.jseaes.2020.104351>, 2020.

Zhang, W., Harff, J., Schneider, R., Meyer, M., Zorita, E., Hünicke, B.: Holocene morphogenesis at the southern Baltic Sea: simulation of multiscale processes and their interactions for the Darss-Zingst peninsula. *Journal of Marine Systems*, 129, 4–18, <https://doi.org/10.1016/j.jmarsys.2013.06.003>, 2014.

905 Zhang, W., Harff, J., Schneider, R., Meyer, M., Wu, C.Y.: A multi-scale centennial morphodynamic model for the southern Baltic coast. *Journal of Coastal Research*, 27, 890–917. <https://doi.org/10.2112/JCOASTRES-D-10-00055.1>, 2011a.

Zhang, W., Harff, J and Schneider, R.: Analysis of 50-year wind data of the southern Baltic Sea for modelling coastal morphological evolution - a case study from the Darss-Zingst Peninsula. *Oceanologia*, 53 (1-TI), 489–518. doi:10.5697/oc.53-1-TI.489, 2011b.

910